HIGH-PRESSURE SPEED OF SOUND IN PURE CO_2 AND IN CO_2 WITH SO_2 AS AN IMPURITY USING METHANOL AS A DOPING AGENT

Clara Rivas, Beatriz Gimeno, Manuela Artal, Sofía T. Blanco, Javier Fernández, Inmaculada Velasco*

Departamento de Química Física, Facultad de Ciencias, Universidad de Zaragoza, 50009 – Zaragoza, Spain

*Corresponding author: curra@unizar.es

ABSTRACT

Reliable speed of sound, *c*, values in CO_2-rich mixtures and pure CO_2 are required for carbon capture and storage (CCS) technology but are difficult to determine, particularly at relatively high frequencies. We tested the suitability of methanol as doping agent to obtain accurate *c* values in CCS systems at 5 MHz. We measured *c* in seven CO_2-rich, CO_2+methanol mixtures between 263.15 and 323.15 K and up to 196.30 MPa, and we extrapolated the values to obtain *c* in pure CO_2. Additionally, we measured *c* from 263.15 to 373.19 K and up to 190.10 MPa in two CO_2-rich, CO_2+SO_2 mixtures with the same SO_2 composition, which is of interest for CCS, with one mixture doped with methanol. We compared our results for pure CO_2 with the literature and the Span and Wagner equation of state (EoS). We validated the PC-SAFT EoS and the modeling with the REFPROP 9 software for the mixtures by comparing the predicted values with our experimental data under the studied conditions. We conclude that methanol is a suitable doping agent to measure *c* in pure CO_2 and CO_2-rich mixtures. For the CO_2+SO_2 mixtures, the effect of methanol on the experimental values is small and negligible for modeling.

Keywords

CCS, speed of sound, CO_2, methanol, dopant, SO_2

1. Introduction

The concentration of CO_2 in the atmosphere increased 2.1 ppm/year during the last ten years, exceeding 400 ppm in March 2015 (Mauna Loa Observatory). This value is 15% higher than the recommended upper limit of 350 ppm to avoid dangerous climate effects (Hansen et al., 2008; Allen et al., 2009). Despite political commitments (KP 1998; UNFCCC 2006, 2008, 2010, 2012, 2014, 2015, 2016), fossil fuels are expected to account for 75% of global energy demand by 2035. Global energy demand is expected to grow, mainly in developing countries, and estimations predict that energy-related CO_2 emissions will increase by 20% in the same period. Such increases will lead to a long-term scenario with an average temperature increase of 3.6°C, far above the 2°C target internationally agreed upon in 2009 and ratified in 2015 (UNFCCC 2010, 2016).

Carbon capture and storage (CCS) technology is a realistic, effective and promising option to significantly reduce large-scale CO_2 emissions. CCS plays an important role in the mitigation of climate change, in combination with increased energy efficiency, fuel switching and the development of renewable energy sources. In the absence of CCS technology, the additional investment needed to meet the 2°C target would increase by at least USD 2 trillion by 2050 (IEA, 2012).

The most economical and operational means of transporting anthropogenic CO_2 from capture and conditioning facilities to geological storage sites is typically through pipelines as a dense-phase fluid (either liquid or supercritical). Pipeline design must be optimized to ensure cost-effectiveness and safety. The speed of sound, c, is a useful property to study several aspects of transport, such as

45 detection and monitoring of (undesired) gas bubbles in the dense phase and depressurization and
46 leak checking, because *c* determines how fast the pressure will drop (Aursand et al., 2013; Leighton
47 et al., 2012; Lund et al., 2011; Medwin, 1977; Stoianov et al., 2007; Zhang, 1996).

48 Because of the conditions inside geologic reservoirs, the fluid is usually in the supercritical phase
49 during storage. In this step, *c* can be used to monitor the formation of bubbles in leakages (Bergès
50 et al., 2015; Leighton and White, 2012**)**, estimate the seismic properties of hydrocarbon reservoirs,
51 optimize enhanced oil recovery (EOR) processes, and monitor CO_2 plumes in saline aquifers and
52 depleted reservoirs (Lebedev et al., 2014; Siggins et al., 2010).

53 Anthropogenic CO_2 is not pure CO_2 but contains impurities that can modify its properties and thus
54 influence its behavior in the different steps of CCS technology. N_2, H_2, O_2, Ar, SO_2, NO_x, CO and
55 water are the main impurities (Løvseth et al., 2013; Porter et al., 2015), and methanol can be
56 present because of its use as a hydrate inhibitor and as a residue from pipeline drying. Recent
57 publications suggest that the presence of certain impurities, such as SO_2, favors some aspects of the
58 CCS process and propose the co-capture of CO_2/SO_2, which additionally avoids SO_2 emissions to the
59 atmosphere (Elshahomi et al., 2015; Koenen et al., 2015; Wang et al., 2015, 2011; Wolf et al., 2015;
60 Ziabakhsh-Ganji and Kooi, 2014a, 2014b). We are conducting a wide range of research on the
61 determination of values for the thermodynamic properties of CO_2-rich mixtures containing SO_2 and
62 other impurities. We are studying the influence of these impurities on CCS parameters for transport
63 and storage to determine the feasibility of CO_2/SO_2 co-capture (Gimeno et al., 2015).

64 Experimental thermodynamic data for the systems and conditions of interest for CCS technology
65 are scarce. For pipeline management and safety, the thermodynamic properties of fluids are often
66 obtained from thermodynamic models, usually equations of state, EoSs (Eiber et al., 1993; Picard

and Bishnoi, 1988; Mahgerefteh et al., 2012a, 2012b). For industrial applications, cubic EoSs are preferred due to their simplicity, but deviations from real behavior are often important, particularly when the fluid contains polar components. Multiparametric approaches, such as GERG EoS (Kunz et al., 2007; Kunz and Wagner, 2012), with good accuracy for mixtures containing compounds included in the database, are difficult to expand to other mixtures, and consume more computer time. PC-SAFT EoSs (Gross and Sadowski, 2001, 2002), which is based on perturbation theory, presents intermediate accuracy and complexity. The shortage of experimental thermodynamic data under conditions relevant to CCS technology complicates EoS validation, and there is no reference model to predict the behavior of the transported and stored fluid (Li et al., 2011).

With respect to pure CO_2, many thermodynamic properties have been accurately determined under wide ranges of temperature and pressure; however, *c* data under CCS conditions are not abundant. The reference EoS for CO_2, SW EoS (Span and Wagner, 1996), collected data from four sources (Herget, 1940; Lemming, 1989; Novikov and Trelin, 1962; Pitaevskaya and Bilevich, 1973), and only those from Pitaevskaya and Bilevich include some temperatures of interest for CCS. More recently, Al-Siyabi (2013) and Lin (2013) reported data under CCS conditions using ultrasonic pulse-echo techniques. Several works have focused on the study of the critical region and/or the use of *c* to determine the critical point of pure CO_2 (Herget, 1940; Kordikowski et al., 1996; Oag et al., 2004; Parbrook and Richardson, 1952; Tielsch and Tanneberger, 1954; Trelin and Sheludyakov, 1966; Zevnik, et al., 2006).

Experimental determination of *c in* pure, dense CO_2 presents serious difficulties due to its high sound absorption, α, associated with its long vibrational relaxation time, τ, which results in poor or no signal detection at relatively high frequencies. τ can be reduced by decreasing the working frequency, but this requires a large volume of fluid (not advisable with high-pressures techniques),

and echoes and diffraction effects can hinder the interpretation of the results (Lin, 2013; Lin and Trusler, 2014). An alternative is the use of a *catalyst* or *dopant*. Knudsen and Fricke (1940) investigated the influence of small amounts of certain impurities (H_2, H_2O, H_2S, CH_3OH, C_3H_7OH and $C_6H_5CH_3$) on the acoustic behavior of highly absorptive gases (CO_2, N_2O, COS and CS_2) at atmospheric pressure and 23°C. They determined that the impurities accelerate the reaction rate of the transition of these gases from vibrating to non-vibrating molecules, decreasing the time of survival of the activated molecules and decreasing both α and τ. In this way, Lin and Trusler (2014) derived c in pure CO_2 based on measurements in mixtures of CO_2 containing small amounts of propane as the dopant at 2 MHz, temperatures between 248 and 373 K and pressures up to 200 MPa. Extrapolation of these measurements to a zero concentration of the dopant enabled the determination of c in pure CO_2.

We utilize a double-path, double-echo, ultrasonic pulse facility that functions at 5 MHz. At this frequency, we obtain no signal or a very poor signal in either pure CO_2 or in several CO_2-rich mixtures of interest for CCS technology, such as CO_2+SO_2 with $x_{CO_2} > 0.9$. In addition, we cannot use propane as a dopant at this frequency (we obtained only a tiny signal for CO_2+C_3H_8 with $x_{CO_2} \cong 0.8$), and thus we must select another doping compound that is adequate for the features of our measurement device. We selected methanol, an impurity studied by Knudsen and Fricke (1940). Methanol is chemically compatible with the installation, has well-known properties as a modifier in supercritical extraction, is used in industrial processes as Rectisol, and is added as a desiccant and/or hydrate inhibitor (Boot-Handford et al., 2014; Dykhno, L. et al., 2011; Esteban et al., 2000; Feng et al., 2014; Kemper et al., 2014; Keresteciogl u and Haberle, 2010; McIntyre et al., 2004; Perry and Eliason, 2004; Peterhead CCS Project, 2015; Weiss and Schriefl, 2010).

112 The aims of this work were as follows: i) to test the suitability of methanol as doping agent to
113 obtain reliable values of *c* at 5 MHz in the working ranges of our installation, not only in doped
114 "pure" dense CO_2 but also in acoustically opaque CO_2-rich mixtures of interest for CCS; ii) to
115 quantify the effect of methanol on *c* in pure CO_2 and in a CO_2+SO_2 mixture of interest for CCS; iii) to
116 validate the PC-SAFT EoS and the modeling implemented in the REFPROP 9 software for *c* in CO_2-
117 rich mixtures with methanol and/or SO_2, thus contributing to the development and improvement of
118 the models needed for the design of processes in CCS technology.

119 For this purpose, we determined *c* in seven CO_2+CH_3OH mixtures with compositions $0.80 < x_{CO_2} <$
120 0.99 at T = 263.15, 298.15 and 323.15 K and up to approximately 200 MPa. By extrapolation of *c* in
121 the five CO_2-richest mixtures to infinite dilution, we obtained reliable values of c in pure CO_2 and
122 compared these results with the literature (Al-Siyabi, 2013; Lin, 2013; Lin and Trusler, 2014;
123 Pitaevskaya and Bilevich, 1973). We estimated the effect of methanol by comparing our results for
124 the mixtures of CO_2+methanol with those calculated using the reference EoS for pure CO_2 (Span
125 and Wagner, 1996). In addition, we compared the results for binary mixtures with those calculated
126 using the PC-SAFT EoS (Gross and Sadowski, 2001, 2002) and the modeling procedure implemented
127 in the REFPROP 9 software (Lemmon et al. 2010). Finally, we applied the doping to a mixture of
128 CO_2+SO_2 with $x_{SO_2} = 0.1031$. We measured *c* in both undoped and doped mixtures of this
129 composition at eight temperatures between 263.15 and 373.19 K and at pressures up to
130 approximately 190 MPa, and we compared the results with each other and with those predicted by
131 the specified models.

132 **2. Materials and methods**

133 *2.1. Chemicals*

Carbon dioxide (mole fraction > 0.99998) and sulfur dioxide (mole fraction 0.9990), from Air Liquide, were used as received. Methanol (biotech. grade, mole fraction 0.9993), from Sigma Aldrich, was degassed immediately before use.

2.2. Apparatus and procedure

Speed of sound measurements were performed using an installation that employs a pulsed ultrasonic system, which allows measurements in liquids and in compressed gases in dense or supercritical phase with viscosities up to around 100 mPa s (Ball and Trusler, 2001; Dávila and Trusler, 2009; Lin and Trusler, 2014). The main component is a dual-path ultrasonic cell located within a pressure vessel inside a thermostatic bath. Both ends of the cell are stainless-steel reflectors, and a piezoceramic transducer of lead zirconate titanate ($PbZrO_3$/$PbTiO_3$) is hold between them, at constant and unequal distances of each one, by means of fused quartz spacers. The transducer is operated at its resonance frequency of 5 MHz. Excited by a single five-cycle tone burst (5 MHz, 10 V peak-to-peak amplitude), the transducer emits ultrasonic pulses that propagate into the fluid to either side. The pulses are reflected by the reflectors at the ends of the cell, and the two returning echoes are detected when they reach the transducer again. The speed of sound in the fluid is determined using $c = 2\Delta L/\Delta t$, where ΔL is the difference between the two path lengths (unequal transducer-reflector distances), determined by previous calibration, and Δt is the difference between the two detection times. The apparatus works from 253.15 K to 473.15 K, and the temperature is measured using a previously calibrated platinum resistor with a standard uncertainty, u_T, of 0.015 K. The pressure is measured with a pressure transducer Paroscientific Model 430K with a standard uncertainty, u_P, of 0.05 MPa, and the maximum achievable pressure is 200 MPa. A more detailed description of the apparatus, its calibration, measurement procedure, and calculation of the accuracy for pure compounds has been published elsewhere (Velasco et al.,

2011). The procedures for preparing mixtures, performing measurements, and calculating measurement uncertainty are described in Rivas et al. (2016). The standard uncertainty of the experimental c, u_c, was calculated using the propagation uncertainty law

$$u_c^2 = [(\partial c/\partial T)_P u_T]^2 + [(\partial c/\partial P)_T u_P]^2 + [(\partial c/\partial x) u_x]^2 + (u_c^*)^2 \quad (1)$$

where u_x and u_c^* are the standard uncertainty of the mole fraction and the standard repeatability uncertainty, respectively, which depend on the studied system (Rivas et al., 2016). For the mixtures in this work, $u_c = 5.9 \times 10^{-4} c$ for CO_2+CH_3OH (Rivas et al., 2016), $u_c = 6.2 \times 10^{-4} c$ for CO_2+SO_2 and $u_c = 8.1 \times 10^{-4} c$ for CO_2+SO_2+CH_3OH. These values lie within the range of standard uncertainties ($3 \times 10^{-4} c$ to $10 \times 10^{-4} c$) obtained by other authors using similar apparatus for liquids and for compressed gases (Ball and Trusler, 2001; Dávila and Trusler, 2009; Lin and Trusler, 2014).

3. Modeling

In this work, we compared our experimental data with those obtained from the PC-SAFT EoS and the REFPROP 9 software.

3.1. PC-SAFT EoS (Gross and Sadowski, 2001, 2002).

The PC-SAFT EoS describes the dimensionless Helmholtz energy, $\tilde{a}$, as the sum of different contributions: ideal-gas (*id*), hard-chain (*hc*), dispersive attraction (*dis*), association (*assoc*), and multipolar interactions (DD, dipole-dipole, QQ, quadrupole-quadrupole, and QD, quadrupole-dipole):

$$\tilde{a} = \tilde{a}^{id} + \tilde{a}^{hc} + \tilde{a}^{dis} + \tilde{a}^{assoc} + (\tilde{a}^{DD} + \tilde{a}^{QQ} + \tilde{a}^{QD}). \quad (2)$$

In this model, three geometric parameters (m, σ, ε) are needed to describe each non-associated and non-polar pure compound. In the mixtures, for each pair of compounds, i and j, classical mixing rules with an adjustable binary interaction parameter, k_{ij}, are used to calculate σ_{ij} and ε_{ij}:

$$\sigma_{ij} = \frac{1}{2}(\sigma_i + \sigma_j); \tag{3}$$

$$\varepsilon_{ij} = \sqrt{\varepsilon_i \varepsilon_j}(1 - k_{ij}). \tag{4}$$

Two additional parameters ($\kappa^{A_iB_i}, \varepsilon^{A_iB_i}$) and an association scheme are required if the molecule is self-associated or undergoes induced association. The latter can be considered in systems containing a self-associated compound and another non-associated compound that possess either proton donor or proton acceptor sites. Then, the cross-association parameters, $\kappa^{A_iB_j}$ and $\varepsilon^{A_iB_j}$, can be calculated from the Kleiner and Sadowski (2007) approach:

$$\kappa^{A_iB_j} = \kappa^{assoc.comp} \qquad \varepsilon^{A_iB_j} = \frac{\varepsilon^{assoc.comp}}{2} \tag{5}$$

In this work, multipolar interactions were not considered, and the calculations were performed using VLXE software (Laursen, 2012).

3.2 REFPROP 9 software (Lemmon et al. 2010).

The software REFPROP (Reference Fluid Thermodynamic and Transport Properties Database) is a program developed by the National Institute of Standards and Technology (NIST) that calculates the thermodynamic and transport properties of fluids of interest and their mixtures. It uses the most accurate pure fluid and mixture models currently available. For the systems studied in this work, we applied the REFPROP 9 version in its "Calculate properties using default equations" option. It uses pure component reference EoSs by different authors, combined with different mixture models. The pure fluid equations are from Span and Wagner (1996) for CO_2, from de Reuck and Craven (1993) for methanol, and from Lemmon and Span (2006) for SO_2. According to Dr. E.W. Lemmon (2016, personal communication), the mixture models use the same functional form as that in the GERG-

2008 EoS (Kunz and Wagner, 2012); apart from their implementation in REFPROP 9, they are unpublished as far as we know. The mixing parameters are available in the REFPROP 9 program.

4. Results

4.1. Speed of sound in the CO_2+CH_3OH system

$P-c-T-x_{CO_2}$measurements for seven CO_2-rich, CO_2+CH_3OH mixtures {x_{CO_2} =0.8005, 0.9025, 0.9503, 0.9700, 0.9794, 0.9845, 0.9898} were performed at 5 MHz and at T= 263.15, 298.15 and 323.15 K, with the exception of $x_{CO_2} = 0.9700$ at 263.15 K, which we published previously (Rivas et al., 2016). For mole fractions $x_{CO_2} > 0.99$, the results for *c* were not reproducible. The maximum pressure for each isotherm and isopleth was delimited by the amount of transferred fluid and the compressibility of the mixture, and the minimum pressure was the lowest at which a clear signal was obtained. The range of pressures was 3.28–196.30 MPa.

The experimental results are listed in Tables 1–3, and their representations are shown in Figs. 1 and S1-S6 (Supplementary Material). For the studied compositions, *c* in the fluid increased with increasing pressure and decreasing temperature. We did not identify speed of sound data in the literature for this system, except data published by ourselves (Rivas et al., 2016), which are in agreement with this work.

The experimental values of *c* were correlated as a function of pressure using the polynomial (Lin and Trusler, 2014)

$$(P - P^{\#}) = \sum_{i=1}^{3} a_i (c - c^{\#})^i, \tag{7}$$

where $P^{\#}$ = 70 MPa and $c^{\#}$ is the speed of sound at $P = P^{\#}$.

The coefficients of equation 7 as well as the mean relative deviations $MRD_c(\%)$ between the fitted and experimental values for each isotherm and isopleth are shown in Table 4. The overall mean relative deviation was $\overline{MRD_c}$ =0.012%, lower than the relative standard uncertainty of the experimental data (0.059%). No clear trends with composition or temperature were observed, with higher deviations at low pressures (Fig. 2).

4.2. Speed of sound in the CO_2+SO_2 and CO_2+CH_3OH+SO_2 systems

To test and quantify the effect of methanol as a doping agent in the CO_2+SO_2 system, we measured eight $P-c-T$ isotherms for each of these systems: a binary mixture with composition x_{CO_2} =0.8969 and x_{SO_2} =0.1031 and a ternary mixture (doped with 0.8% of methanol) with composition x_{CO_2} = 0.8889, x_{CH_3OH} = 0.0080 and x_{SO_2} = 0.1031. The measurements were performed at 263.15, 273.15, 293.15, 304.16, 313.15, 333.15, 353.15 and 373.19 K and from 7.99 to 150.00 MPa for the binary mixture and from 8.00 to 190.10 MPa for the ternary mixture. The amount of CO_2 is sufficiently high to be of interest for CCS, and both mixtures provided reliable values of *c* under the studied conditions. All experimental results are presented in Tables 5 and 6, and values at select temperatures are presented in Figures 3 and 4. The value of *c* increased with increasing pressure and decreasing temperature. No data were identified in the literature on *c* in these mixtures.

The experimental results of *c* for each isotherm and isopleth were correlated to the polynomial (7). Tables 7 and 8 present the values used for $P^{\#}$, the fitting coefficients, and the mean relative deviations for the binary (undoped) and ternary (doped) mixtures, respectively. The overall mean relative deviations of the fittings were 0.025% and 0.010%, respectively, lower than the corresponding relative standard uncertainties of the experimental data (0.062% and 0.081%).

5. Discussion

5.1. Estimated speed of sound in dense, pure CO_2

Dense-phase pure CO_2 exhibits a very long vibrational relaxation time, $\tau_{CO_2-CO_2} \cong 1.71\times10^{-8}$ s, at 298 K and 69 atm (Bass and Lamb, 1958) and a high absorption coefficient at high frequencies. The absorption coefficient of pure CO_2 at several pressures and temperatures can be calculated using the equations collected by Lin and Trusler (2014). Under our working conditions, $\alpha \cong$ 100-1850 m^{-1}, far from the upper detection threshold of our device ($\alpha \cong 40$ m^{-1}); CO_2 is opaque in our facility. However, we can use the catalytic effect of methanol in the deactivation of the vibrating CO_2 molecules (Knudsen et al., 1940): a vibrating CO_2 molecule will survive, on average, 86,000 collisions with other CO_2 molecules at room conditions but only 36 collisions with methanol molecules. In this way, both α and τ decrease significantly.

In this work, we utilized the experimental values of c in the five CO_2-richest, CO_2+methanol mixtures, $x_{CO_2} > 0.95$, and those for the mixture of composition x_{CO_2} =0.9700 at 263.15 K previously determined by us (Rivas et al., 2016) to estimate the values of c in pure CO_2 by extrapolation to $x_{CO_2} = 1$. For this purpose, we used the coefficients from Table 4 to obtain c_{fit} data at round values of P at each T. These interpolated values were correlated as a function of the CO_2 mole fraction (Lin and Trusler, 2014):

$$c_{fit}\left(x_{CO_2}\right) = c_0 + c_1\left(1 - x_{CO_2}\right) + c_2\left(1 - x_{CO_2}\right)^2, \quad (8)$$

where $c_{fit}\left(x_{CO_2} = 1\right) = c_0$ is the speed of sound in pure CO_2. Table 9 presents the correlated values of c_{fit} and, for each correlation, the coefficients of eq. (8), including the value obtained for c_0 and the standard relative uncertainty of c_0, $u_r(c_0)$. This uncertainty was calculated by combining the relative standard uncertainty of the experimental c, 0.059% (Rivas et al., 2016), with the

257 relative standard deviation of c_0 determined by eq. (8). The overall value, $\overline{u_r(c_0)} = 0.12\%$, is similar
258 to that obtained by Lin and Trusler (2014) using the same procedure but with a different dopant
259 (propane) and frequency (2 MHz) and lower than the tolerance margin (0.5-2%) presented by the
260 SW EoS in this region (Span and Wagner, 1996).

261 In the literature, experimental data on *c* in pure CO_2 under the same conditions as in this work are
262 scarce. Pitaevskaya and Bilevich (1973) determined c at temperatures T=298–473 K and pressures
263 P = 50–450 MPa and reported a minimum accuracy of the speed-density equations of 1%. Lin
264 (2013) measured c at 263–363 K and pressures up to 325 MPa but did not obtain confident values
265 for the uncertainty. Both studies are in good agreement with our results, with overall mean relative
266 deviations $\overline{MRD_c} = 0.61\%$ and $\overline{MRD_c} = 0.44\%$, respectively, when the results at identical
267 temperatures are compared. Al-Siyabi (2013) reported values of c at T=268–301 K and P=3.6–42
268 MPa with an accuracy of ± 1 m/s; these results are consistent with ours but are not directly
269 comparable because they were measured at different temperatures. In addition, we compared our
270 results with those derived by Lin and Trusler (2014) at the same temperatures using propane as a
271 dopant at 2 MHz, obtaining $\overline{MRD_c}$ =0.21%. Comparing our results with the values provided by SW
272 EoS, the difference is $\overline{MRD_c}$ =0.43%. As shown in Fig. 5 and 6, there is good agreement between
273 the whole sets of data. Fig. 7 presents the relative deviations between the literature and this work
274 for *c* in pure CO_2 and those calculated by the SW EoS. The deviations are lower than the tolerance
275 margin of the Span and Wagner equation under these conditions (0.5–2%).

276 *5.2. Quantification of the doping effect of methanol in dense, pure CO_2*

277 Figure 8 presents the mean relative deviations of our experimental values of *c* in the CO_2+methanol
278 mixtures from the values calculated in pure CO_2 using the SW equation, i.e., the error when the
279 mixtures are considered as pure CO_2. For doping at up to 5 mole %, the relative deviations range

from -1.31% to +0.72%, with a $\overline{MRD_c}$ of 0.52%. Doping with only 1 mole % of methanol, the sound echoes are clear at 5 MHz in the studied ranges of pressure and temperature, with relative deviations between -0.82% and +0.52% and $\overline{MRD_c}$ =0.38%. These deviations are higher than the experimental relative standard uncertainty of *c* (0.059%) but are almost always within the tolerance margin of the SW equation. Only three of the entire set of experimental points are slightly outside the tolerance margins, and all three are at low pressures (below 10 MPa), low temperature (263.15 K) and high concentrations of methanol.

Figure 9 shows the correlation of the speed of sound as a function of the composition (equation 8, Table 9) at the three studied temperatures and at several pressures. At 263.15 K, every plot (at each of the pressures of Table 9) presents a minimum between $x_{\mathrm{CO_2}}$=0.960 and 0.962, inside the studied high-dilution interval ($x_{\mathrm{CO_2}}$>0.950). At 298.15 K, the plots show either minima (at $P \leq 80$ MPa) or maxima (at $P \geq 100$ MPa), being all of them out of the high-dilution interval. Inside this interval, *c* increases when the mole fraction of CO_2 increases for all the plots. At 323.15 K, every plot presents a maximum inside the high-dilution interval, between $x_{\mathrm{CO_2}}$ = 0.963 and 0.972. When comparing each derived speed of sound in pure CO_2, c_0, with the minimum (at 263.15 K), the maximum (at 323.15 K) or the most different value of *c* inside the interval (at 298.15 K), we found that $\overline{MRD_c}$ =0.86%, again within the tolerance margin of the SW equation.

5.3. Validation of the PC-SAFT EoS and the REFPROP 9 software for the CO_2+CH_3OH system

A detailed explanation of the application of the PC-SAFT EoS to CO_2+methanol is given in previous works (Gil et al., 2012; Rivas et al., 2016) in which we studied vapor-liquid equilibrium, critical locus, density and *c* over a wide range of temperature and pressure. In these papers, (i) the geometric parameters of the pure compounds were obtained from their critical points; (ii) 2C and 2B association schemes were used for CO_2 and methanol, respectively; (iii) volume translation was

included for the density modeling; and (iv) a temperature-dependent binary interaction parameter was necessary. In this work, we maintained the same procedure, and the values of the parameters used are listed in Table S1.

Table 10 reports the mean relative deviations between our experimental data and those calculated using the two models (PC-SAFT and REFPROP 9). Figures 1 and S1-S6 present our experimental results along with the calculated values for each composition and temperature. The relative deviations between the experimental and calculated values are presented in Fig. S7-S9.

The PC-SAFT EoS relative deviations for each mole fraction and temperature become nearly constant at pressures above approximately 50 MPa at 263.15 K and 90 MPa at 298.15 and 323.15 K; in this region, the deviations increase with increasing CO_2 concentration. At low pressures, the differences are higher at lower concentrations of CO_2 at 298.15 and 323.15 K. The relative deviations obtained using this model range from -5.21% to +11.4%, with an overall value of $\overline{MRD_c}$ =2.83%.

The REFPROP 9 software overestimates *c* at all studied temperatures, pressures and compositions, with higher deviations at lower working pressures and higher concentrations of methanol. The relative deviations range from 0.3% to 26.3%, and the overall mean relative deviation is $\overline{MRD_c}$ =4.97%. However, the REFPROP 9 deviations decrease significantly with increasing CO_2, and for the three CO_2-richest mixtures, $\overline{MRD_c}$ is 1.23%.

5.4. Effect of methanol on c *in a mixture of CO_2+SO_2*

To assess the usefulness of doping in a CO_2-rich mixture of interest for CCS, we used the system CO_2+SO_2. We prepared two mixtures, one without methanol, with composition x_{CO_2} =0.8969 and x_{SO_2} =0.1031, and the other doped with 0.8 mole % methanol, x_{CO_2} =0.8889, x_{CH_3OH} =0.0080 and

325 x_{SO_2} =0.1031. The amount of methanol was 0.8%, which is lower than the amount required for
326 detecting a signal in pure CO_2 in our facility (Section 4.1). We observed that SO_2 favors the
327 deactivation of the vibrating CO_2 molecules. The value of *c* at 5 MHz was measured in both mixtures
328 at eight temperatures between 263.15 and 373.19 K and an overall range of pressures from 7.99 to
329 190.10 MPa. We obtained good signals in both mixtures in these ranges, which permitted
330 comparison to quantify the effect of methanol on the experimental values of *c*.

331 To compare the results for both mixtures, we extrapolated the experimental values of *c* in the
332 binary mixture at each *T* up to 190.0 MPa using equation (7) and the coefficients from Table 7. The
333 relative deviations are between -0.96% and +0.29% (Fig. 10). These deviations are similar to those
334 for the CO_2+CH_3OH(1%) mixture (section 5.2, Fig. 8). The overall mean relative deviation is only
335 0.17%, less than half that of the last mixture value (0.38%) and approximately twice the
336 experimental relative standard uncertainty of the measurements for the ternary mixture (0.081%).
337 The trend of the deviations with temperature is not clear, and larger differences are observed at
338 low pressures.

339 *5.5. Validation of the PC-SAFT EoS and the REFPROP 9 software for the CO_2+SO_2 and*
340 *CO_2+CH_3OH+SO_2 mixtures*

341 The CO_2+SO_2 system (two non-associated compounds) was modeled with the PC-SAFT EoS using the
342 original parameters from Gross and Sadowski (2001) and the binary interaction parameter
343 published by Diamantonis et al. (2013) (Table S1).

344 Both models, PC-SAFT and REFPROP 9, adequately predict *c* in this mixture (Table 11), but the
345 trends with pressure are opposite (Figures 3 and S10). The overall mean relative deviation using PC-
346 SAFT is $\overline{MRD_c}$ =2.19%, and the deviation increases with increasing pressure. However, REFPROP 9

results in higher deviations at lower pressures, with $\overline{MRD_c}$ =1.39%. For both models, higher deviations are observed at lower temperatures.

The CO_2+CH_3OH+SO_2 mixture was modeled in two different ways:

(a) Considering the actual composition of the ternary mixture (x_{CO_2}=0.8889, x_{CH_3OH}=0.0080, x_{SO_2}=0.1031). Modeling with PC-SAFT EoS, the pure compound parameters for CO_2 and CH_3OH and its interaction binary parameter, k_{ij}(CO_2-CH_3OH), were as described in section 5.3 (mixture CO_2+CH_3OH). The pure compound parameters for SO_2 and the CO_2-SO_2 binary interaction parameter were taken from the literature, as described above (mixture CO_2+SO_2). It was assumed k_{ij}(SO_2-CH_3OH)=0 due to the small amount of both compounds in the mixture. The parameters are presented in Table S1. The deviations obtained for modeling this mixture as a ternary mixture are presented in Table 11 and Figures S11 and S12. By comparing our data with the PC-SAFT calculated values, we obtained an overall $\overline{MRD_c}$ =3.24%, and the observed deviations decrease with increasing temperature. From REFPROP 9, the overall $\overline{MRD_c}$ =1.28%, and the deviations are higher at low temperatures and pressures.

(b) Considering the ternary mixture as a binary mixture in which the methanol mole fraction is added to that of CO_2 (x_{CO_2}=0.8889+0.0080; x_{SO_2}=0.1031). Both models were applied using the same procedure described above for the CO_2+SO_2 mixture. The deviations obtained are presented in Table 11 and Figures 4 and S13. The overall deviations obtained using PC-SAFT and REFPROP 9 were $\overline{MRD_c}$ =2.35% and 1.26%, respectively. The trends with P and T are similar to those observed in (a).

Regarding the variation of the relative deviations with pressure, for both methods of modeling, (a) and (b), both models exhibited opposite trends (Fig. S12 and S13). Similar behavior was observed in the CO_2+SO_2 mixture (Fig. S10).

PC-SAFT more accurately reproduces the experimental results of the ternary mixture if it is modeled as binary rather than as ternary, whereas REFPROP 9 produces similar results for binary and ternary modeling.

6. Conclusions

Due to the great difficulties in determining *c* in pure CO_2 and in many CO_2-rich mixtures of interest for CCS, we evaluated the suitability of methanol as a doping agent at a frequency of 5 MHz. The addition of methanol between 1% and 5% to pure CO_2 enabled the measurement of *c* at the cited frequency in the studied ranges of pressure and temperature. This effect was studied by the measurement of *c* in seven CO_2+methanol mixtures with $0.8005 < x_{CO_2} < 0.9898$ at temperatures *T*=263.15, 298.15 and 323.15 K at a global pressure range of 3.28–196.30 MPa. The standard uncertainty of the experimental results, $u_c = 5.9 \times 10^{-4} c$, is within the values reported in the literature. By extrapolation of the experimental results to $x_{CO_2} = 1$, we obtained *c* in pure CO_2. The derived results exhibited deviations between 0.21% and 0.61% from the literature data and of 0.43% from the Span and Wagner EoS for pure CO_2. The quantification of the doping effect was estimated by calculating the error in *c* if the mixtures were considered pure CO_2. When doping with 1% methanol, we obtained reproducible measures and $\overline{MRD_c}$ =0.38% with respect to pure CO_2 (Span and Wagner EoS). These deviations are within the tolerance margin of the Span and Wagner equation under the studied conditions (0.5–2%).

389 The experimental results of the mixtures were compared with those calculated using the PC-SAFT
390 EoS and the REFPROP 9 software, resulting in $\overline{MRD_c}$ of 2.83% and 4.97%, respectively. The
391 differences with REFPROP 9 decrease significantly with increasing CO_2 and are 11.9% for
392 $x_{CO_2} = 0.8005$ and only 1.23%, on average, for the three CO_2-richest compositions.

393 The effect of methanol on the mixture of interest for CCS technology was studied by comparing the
394 *c* results for two CO_2+SO_2 (binary, undoped) and CO_2+CH_3OH+SO_2 (ternary, doped) mixtures with
395 the same SO_2 mole fraction ($x_{SO_2} = 0.1031$) containing 0.8% methanol. The working temperature
396 and pressure ranged from 263.15 to 373.19 K and from 7.99 to 190.10 MPa. The experimental
397 standard uncertainties were $u_c = 6.2 \times 10^{-4} c$ for the undoped mixture and $u_c = 8.1 \times 10^{-4} c$ for
398 the doped mixture.

399 When comparing the *c* results for both mixtures, we observed that the overall mean relative
400 deviation was $\overline{MRD_c}$ =0.17%, approximately half that observed when 1% methanol was added to
401 pure CO_2 (0.38%) and approximately twice the experimental relative standard uncertainty of *c* in
402 the CO_2+CH_3OH+SO_2 mixtures (0.081%).

403 Both mixtures were modeled with PC-SAFT EoS and REFPROP 9 software, and the following overall
404 mean relative deviations were obtained: 2.19% and 1.39%, respectively, for the binary mixture and
405 3.24% and 1.28%, respectively, for the ternary (doped) mixture. When the ternary mixture was
406 modeled as if it was a binary mixture, the deviations were 2.35% with PC-SAFT and 1.26% with
407 REFPROP 9.

408 We verified the suitability of methanol as a doping agent to obtain reliable values of *c* at 5 MHz in
409 pure dense CO_2 and in a CO_2+SO_2 mixture of interest for CCS. Moreover, we have also quantified
410 the effect of methanol on *c* in these systems. The effect of methanol on the experimental values is

small, and the effect of methanol on modeling is negligible. These results will allow us to obtain reliable values of *c* in CO_2-rich mixtures that would otherwise not be possible.

Acknowledgements

This research received funding from the Ministry of Economy and Competitiveness of Spain ENE2013-44336-R and from the Government of Aragon and the European Social Fund.

Appendix A. Supplementary material

Supplementary material for this article can be found in the online version. Table S1 contains the parameters used in the PC-SAFT modeling. Figures S1-S6 and S11 present the experimental and modeled speeds of sound in the studied mixtures. Figures S7-S10, S12 and S13 show the relative deviations between the experimental and modeled speeds of sound in the studied mixtures.

References

Allen, M.R., Frame, D.J., Huntingford, C., Jones, C.D., Lowe, J.A., Meinshausen, M., Meinshausen, N., 2009. Warming caused by cumulative carbon emissions towards the trillionth tonne. Nature, 458, 1163-1166. http://dx.doi.org/10.1038/nature08019.

Al-Siyabi, I., 2013. Effect of impurities on CO_2 stream properties, Ph.D. Thesis. Heriot Watt University, Edinburg, U.K.

Aursand, P., Hammer, M., Munkejord, S.T., Wilhelmsen, O., 2013. Pipeline transport of CO_2 mixtures: Models for transient simulation. International Journal of Greenhouse Gas Control 15, 174–185. http://dx.doi.org/10.1016/j.ijggc.2013.02.012.

Ball, S.J., Trusler, J.P.M., 2001. Speed of sound of *n*-hexane and *n*-hexadecane at temperatures detween 298 and 373 K and pressures up to 100 MPa. International Journal of Thermophysics 22, 427-443. http://dx.doi.org/10.1023/A:1010770730612.

Bass, R., Lamb, J., 1958. Ultrasonic relaxation of the vibrational specific heat of carbon dioxide, sulphur hexafluoride, nitrous oxide, *cyclo*propane and methyl chloride in the liquid state. Proceedings of the Royal Society of London Series A 247, 168-185. http://dx.doi.org/10.1098/rspa.1958.0176.

Bergès, B.J.P., Leighton, T.G., White, P.R., 2015. Passive acoustic quantification of gas fluxes during controlled gas release experiments. International Journal of Greenhouse Gas Control 38, 64-79. http://dx.doi.org/10.1016/j.ijggc.2015.02.008.

Boot-Handford, M.E., Abanades, J.C., Anthony, E.J., Blunt, M.J.,Brandani, S., MacDowell, N., Fernández, J.R., Ferrari, M.C., Gross, R., Hallett, J.P., Haszeldine, R.S., Heptonstall, P., Lyngfelt, A., Makuch, Z., Mangano, E., Porter, R.T.J., Pourkashanian, M., Rochelle, G.T., Shah, N., Yaoa, J.G., Fennell, P.S., 2014. Carbon capture and storage update. Energy & Environmental Science 7, 130-189. http://dx.doi.org/10.1039/c3ee42350f.

Dávila, M.J., Trusler, J.P.M., 2009. Thermodynamic properties of mixtures of *N*-methyl-2-pyrrolidinone and methanol at temperatures between 298.15 K and 343.15 K and pressures up to 60 MPa. Journal of Chemical Thermodynamics 41, 35-45. http://dx.doi.org/10.1016/j.jct.2008.08.003.

de Reuck, K.M., Craven, R.J.B., 1993. Methanol, International Thermodynamic Tables of the Fluid State – 12. IUPAC, Blackwell Scientific Publications, London.

Diamantonis, N.I., Boulougouris, G.C., Mansoor, E.,Tsangaris, D.M., Economou, I.G., 2013. Evaluation of cubic, SAFT, and PC-SAFT equations of state for the vapor-liquid equilibrium modeling of CO_2 mixtures with other gases. Industrial & Engineering Chemistry Research 52, 3933-3942. http://dx.doi.org/10.1021/ie303248q.

Dykhno, L., 2011. Quest CCS Project: Quest pipelines flow and flow assurance design and operatibility report. 07-2-LA-5507-0003.

Eiber, R.J., Bubenik, T.A., Maxey, W.A., 1993. GASDECOM: Computer code for the calculation of gas decompression speed that is included in fracture control technology for natural gas pipelines. NG-18 Report 208. American Gas Association Catalog N L51691.

460 Elshahomi, A., Lu, Ch., Michal, G., Liu, X., Godbole, A., Venton, P., 2015. Decompression wave speed
461 in CO_2 mixtures: CFD modelling with the GERG-2008 equation of state. Applied Energy 140, 20–32.
462 http://dx.doi.org/10.1016/j.apenergy.2014.11.054.

463 Esteban, A., Hernández, V., Lunsfor, K., 2000. Exploit the benefits of metanol. Proceedings of 79th
464 GPA Annual Convention, Atlanta, USA.

465 Feng, Y., Hu, S., Liu, X., Luo, G., Zhu, G., 2014. Prevention and disposal technologies of gas hydrates
466 in high-sulfur gas reservoirs containing CO_2. Journal of Natural Gas Science and Engineering 19, 344-
467 349. http://dx.doi.org/10.1016/j.jngse.2014.05.024.

468 Gil, L., Blanco, S., Rivas, C., Laga, E., Fernández, J., Artal, M., Velasco, I., 2012. Experimental
469 determination of the critical loci for {*n*-C6H14 or CO2 + alkan-1-ol} mixtures. Evaluation of their
470 critical and subcritical behavior using PC-SAFT EoS. The Journal of Supercritical Fluids 71, 26-44.
471 http://dx.doi.org/10.1016/j.supflu.2012.07.008.

472 Gimeno, B., Fernández, J., Artal, M., Blanco, S.T., Velasco. I., 2015. CO_2 +SO_2 co-capture assessment.
473 Part. 1. International Forum on Recent Developments of CCS Implementations. Athens, 26th-27th
474 March.

475 Gross, J., Sadowski, G., 2001. Perturbed-Chain SAFT: An Equation of State Based on a Perturbation
476 Theory for Chain Molecules. Industrial & Engineering Chemical Research 40, 1244-1260.
477 http://dx.doi.org/10.1021/ie0003887.

478 Gross, J., Sadowski, G., 2002. Application of the Perturbed-Chain SAFT equation of state to
479 associating systems. Industrial & Engineering Chemical Research 41, 5510-5515.
480 http://dx.doi.org/10.1021/ie010954d.

481 Hansen, J., Sato, M., Kharecha, P., Beerling, D., Berner, R., Masson-Delmotte, V., Pagani, M., Raymo,
482 M., Royer, D.L., Zachos, J.C., 2008. Target atmospheric CO_2: Where should humanity aim? The Open
483 Atmospheric Science Journal 2, 217-231. http://dx.doi.org/10.2174/1874282300802010217.

484 Herget, C.M., 1940. Ultrasonic velocity in carbon dioxide and ethylene in the critical region. The
485 Journal of Chemical Physics 8, 537-542. http://dx.doi.org/10.1063/1.1750708.

IEA, 2012. Energy Technology Perspectives. Pathways to a clean energy system. https://www.iea.org/publications/freepublications/publication/energy-technology-perspectives-2012.html

Kemper, J., Sutherland, L., Watt, J., Santos, S., 2014. Evaluation and analysis of the performance of dehydration units for CO_2 capture. Energy Procedia 63, 7568 – 7584. http://dx.doi.org/10.1016/j.egypro.2014.11.792.

Keresteciogl u, U., Haberle, T., 2010. Rectisol® Wash Units. Acid gas removal for polygeneration concepts downstream gasification. GTC Conference, Washington DC, USA.

Kleiner, M., Sadowski, G., 2007. Modeling of polar systems using PCP-SAFT: An approach to account for induced-association interactions. Journal of Physical Chemistry 111, 15544-15553. http://dx.doi.org/10.1021/jp072640v.

Knudsen, V.O., Fricke, E., 1940. The absorption of sound in CO_2, N_2O, COS, and in CS_2, containing added impurities. Journal of the Acoustic Society of America 12, 255-259. http://dx.doi.org/10.1121/1.1916099.

Koenen, M., Waldmann, S., Hofstee, C., Neele, F., 2015. Effect of SO_2 co-injection on CO_2 storage. 2nd International Forum on Recent Developments of CCS Implementations. Athens, 16th-17th December.

Kordikowski, A., Robertson, D.G., Aguiar-Ricardo, A.I., Popov, V.K., Howdle, S.M., Poliakoff, M., 1996. Probing vapor/liquid-equilibria of near-critical mixtures by acoustic measurements. The Journal of Physical Chemistry 100, 9522-9526. http://dx.doi.org/10.1021/jp960010f.

KP, 1998. Kyoto Protocol to the United Nations Framework Convention on Climate Change. http://unfccc.int/resource/docs/convkp/kpeng.pdf.

Kunz, O., Klimeck, R., Wagner, W., Jaeschke, M., 2007. The GERG-2004 wide-range equation of state for natural gases and other mixtures; GERG TM15; Fortschr.-Ber. VDI, Reihe 6, Nr. 557, VDI Verlag: Düsseldorf.

511 Kunz, O., Wagner, W., 2012. The GERG-2008 Wide-Range Equation of State for Natural Gases and
512 Other Mixtures: An Expansion of GERG-2004. Journal of Chemical & Engineering Data 57, 3032-
513 3091. http://dx.doi.org/10.1021/je300655b.

514 Laursen, T. VLXE ApS. Scion-DTU, Diplomvej, Denmark, 2012.

515 Lebedev, M., Bilenko, O., Mikhaltsevitch, V., Pervukhina, M., Gurevich, B., 2014. Laboratory
516 measurements of ultrasonic velocities in CO_2 saturated brines. Energy Procedia 63, 4273 – 4280.
517 http://dx.doi.org/10.1016/j.egypro.2014.11.462.

518 Leighton, T.G., Baik, K., Jiang, J., 2012. The use of acoustic inversion to estimate the bubble size
519 distribution in pipelines. Proceedings of the Royal Society A 468, 2461-2484.
520 http://dx.doi.org/10.1098/rspa.2012.0053.

521 Leighton, T.G., White, P.R., 2012. Quantification of undersea gas leaks from carbon capture and
522 storage facilities, from pipelines and from methane seeps, by their acoustic emissions. Proceedings
523 of the Royal Society A 468, 485-510. http://dx.doi.org/10.1098/rspa.2011.0221.

524 Lemming, W., 1989. Experimentelle Bestimmung akustischer und thermischer Virialkoeffizienten
525 von Arbeitsstoffen der Energietechnik. VDI Forstschritt-Berichte, Reihe 19, Nr. 32.

526 Lemmon, E. W., Huber, M. L., McLinden, M. O., 2010. NIST Standard Reference Database
527 23: Reference Fluid Thermodynamic and Transport Properties-REFPROP, Version 9.0, National
528 Institute of Standards and Technology, Standard Reference Data Program, Gaithersburg.

529 Lemmon, E.W.; Span, R., 2006. Short Fundamental Equations of State for 20 Industrial Fluids.
530 Journal of Chemical and Engineering Data 51, 785-850. http://dx.doi.org/10.1021/je050186n.

531 Li, H., Jakobsen, J.P., Wilhelmsen, Ø., Yan, J., 2011. PVTxy properties of CO_2 mixtures relevant for
532 CO_2 capture, transport and storage: Review of available experimental data and theoretical models.
533 Applied Energy, 88, 3567-3579. http://dx.doi.org/10.1016/j.apenergy.2011.03.052.

534 Lin, C.W., 2013. Thermophysical properties of industrial fluids at high pressures from sound speed
535 and density measurements. Ph.D. Thesis, Imperial College, London, U.K.

536 Lin, C.W., Trusler, J.P.M., 2014. Speed of sound in (carbon dioxide + propane) and derived sound
537 speed of pure carbon dioxide at temperatures between (248 and 373) K and at pressures up to 200
538 MPa. Journal of Chemical & Engineering Data 59, 4099-4109. http://dx.doi.org/10.1021/je5007407.

539 Løvseth, S.W., Skaugen, G., Jacob Stang, H.G., Jakobsen, J.P., Wilhelmsen, Ø., Span, R., Wegge, R.,
540 2013. CO_2Mix Project: Experimental determination of thermo physical properties of CO_2 −rich
541 mixtures. Energy Procedia, 37, 2888–2896. doi: 10.1016/j.egypro.2013.06.174.

542 Lund, H., Flatten, T., Munkejord, S.T., 2011. Depressurization of carbon dioxide in pipelines –
543 models and methods, Energy Procedia 4, 2984–2991.
544 http://dx.doi.org/10.1016/j.egypro.2011.02.208.

545 Mahgerefteh, H., Brown, S., Denton, G., 2012a. Modelling the impact of stream impurities on
546 ductile fractures in CO_2 pipelines. Chemical Engineering Science 74, 200–210.
547 http://dx.doi.org/10.1016/j.ces.2012.02.037.

548 Mahgerefteh, H., Brown, S., Martynov, S., 2012b. A study of the effects of friction, heat transfer,
549 and stream impurities on the decompression behavior in CO_2 pipelines. Greenhouse Gases: Science
550 and Technology 2, 369–379. http://dx.doi.org/10.1002/ghg.1302.

551 Mauna Loa Observatory, Scripps Institution of Oceanography. http://co2now.org/.

552 McIntyre, G., Hlavinka, M., Hernandez, V., 2004. Hydrate Inhibition with Methanol—A Review and
553 New Concerns over Experimental Data Presentation. Proceedings of 83rd GPA Annual Convention,
554 New Orleans, USA.

555 Medwin, H., 1977. Counting bubbles acoustically – Review. Ultrasonics 15, 7-13.
556 http://dx.doi.org/10.1016/0041-624X(77)90005-1.

557 Novikov , L.I., Trelin, Y.S., 1962. Teploenergetica 9, 78-79.

558 National Institute of Standards and Technology (NIST). https://www.nist.gov.

559 Oag, R.M., King, P.J., Mellor, C.J., George, M.W., Ke, J., Poliakoff, M., Popov, V.K., Bagratashvili, V.N.,
560 2004. Determining phase boundaries and vapour/liquid critical points in supercritical fluids: a multi-

technique approach. The Journal of Supercritical Fluids 30, 259-272. http://dx.doi.org/10.1016/j.supflu.2003.09.021.

Parbrook, H.D., Richardson, E.G., 1952. Propagation of ultrasonic waves in vapours near the critical point. Proceedings of the Physical Society B 65, 437-444. http://dx.doi.org/10.1088/0370-1301/65/6/307.

Perry, M., Eliason, D., 2004. CO_2 recovery and sequestration at Dakota Gasification Company Inc., Technical report, Gasification Technology Conference. http://gasification.org.

Peterhead CCS Project, 2015. Well operation guidelines. Doc. No. PCCS-05-PT-ZR-7180-00003. Shell U.K. Limited.

Picard, D.J., Bishnoi, P.R., 1988. The Importance of real-fluid behavior and non-isentropic effects in modeling decompression characteristics of pipeline fluids for application in ductile fracture propagation analysis. The Canadian Journal of Chemical Engineering 66, 3–12.

Pitaevskaya, L.L., Bilevich, A.V., 1973. The velocity of ultrasound in carbon dioxide at pressures us to 4.5 kbar. Russian Journal of Physical Chemistry 47, 126-127.

Porter, R.T.J., Fairweather, M., Pourkashanian, M., Woolley, R.M., 2015. The range and level of impurities in CO_2 streams from different carbon capture sources. International Journal of Greenhouse Gas Control, 36, 161–174. http://dx.doi.org/10.1016/j.ijggc.2015.02.016.

REFPROP (NIST). https://www.nist.gov/srd/refprop.

Rivas, C., Gimeno, B., Bravo, R., Artal, M., Fernández, J., Blanco, S.T., Velasco, M.I., 2016. Thermodynamic properties of a CO2-rich mixture (CO2+CH3OH) in conditions of interest for carbon dioxide capture and storage technology and other applications. Journal of Chemical Thermodynamics 98, 272-281. http://dx.doi.org/10.1016/j.jct.2016.03.026.

Siggins, A.F., Lwin, M., Wisman, P., 2010. Laboratory calibration of the seismo-acoustic response of CO_2 saturated sandstones. International Journal of Greenhouse Gas Control 4, 920-927. http://dx.doi.org/10.1016/j.ijggc.2010.06.007.

586 Span, R., Wagner, W., 1996. A new equation of state for carbon dioxide covering the fluid region
587 from the triple-point temperature to 1100 K at pressures up to 800 MPa. Journal of Physical and
588 Chemical Reference Data 25, 1509−1596.

589 Stoianov, I., Nachman, L., Madden, S, Tokmouline, T., 2007. PIPENET: A wireless sensor network for
590 pipeline monitoring. Proceedings of the 6th International Conference on Information Processing in
591 Sensor Networks; Cambridge, MA, USA, 264–273. http://dx.doi.org/10.1145/1236360.1236396.

592 Tielsch, H., Tanneberger, H., 1954. Ultraschallausbreitung in Kohlensäure in der Nähe des kritischen
593 Punktes. Zeitschrift für Physik 137, 256-264. http://dx.doi.org/10.1007/BF01328882**.**

594 Trelin, Y.S., Sheludyakov, E.P., 1966. Experimental determination of the speed of sound in the
595 critical region of carbon dioxide. Journal of Experimental and Theoretical Physics Letters 3, 63-64.

596 UNFCCC, 2006. Report of the Conference of the Parties on its eleventh Session. Montreal
597 (FCCC/CP/2005/5).

598 UNFCCC, 2008. Report of the Conference of the Parties on its Thirteenth Session. Bali
599 (FCCC/CP/2007/6).

600 UNFCCC, 2010. Report of the Conference of the Parties on its Fifteenth Session. Copenhagen
601 (FCCC/CP/2009/7).

602 UNFCCC, 2012. Report of the Conference of the Parties on its seventeenth session. Durban
603 (FCCC/CP/2011/9).

604 UNFCCC, 2014. Report of the Conference of the Parties on its nineteenth session. Warsaw
605 (FCCC/CP/2013/10).

606 UNFCCC, 2015. Report of the Conference of the Parties on its twentieth session. Lima
607 (FCCC/CP/2014/10).

608 UNFCCC, 2016. Report of the Conference of the Parties on its twenty-first session. Paris
609 (FCCC/CP/2015/L.9.Rev.1).

610 Velasco, I., Rivas, C., Martínez-López, J. F., Blanco, S. T., Otín, S., Artal, M., 2011. Accurate values of
611 some thermodynamic properties for carbon dioxide, ethane, propane, and some binary mixtures.
612 The Journal of Physical Chemistry B 115, 8216-8230. http://dx.doi.org/10.1021/jp202317n.

613 Wang, J., Ryan, D., Anthony, E.J., Wildgust, N., Aiken, T., 2011. Effects of impurities on CO_2
614 transport, injection and storage. Energy Procedia 4, 3071-3078.
615 http://dx.doi.org/10.1016/j.egypro.2011.02.219.

616 Wang, J., Wang, Z., Ryan, D., Lan, C., 2015. A study of the effect of impurities on CO_2 storage
617 capacity in geological formations. International Journal of Greenhouse Gas Control 424, 132-137.
618 http://dx.doi.org/10.1016/j.ijggc.2015.08.002.

619 Weiss, M.M., Schriefl, A., 2010. Rectisol and oxyclaus: mature processes still going strong.
620 Proceedings of the 10th European Gasification Conference, Amsterdam, The Netherlands.

621 Wolf, J.L., Fischer, S., Waldmann, S., Rütters, H., Niemi, A., Bensabat, J., May, F., Rebscher, D., 2015.
622 Comparison of different numerical and modelling approaches for implementing SO_2 as a flue gas
623 impurity in geochemical simulations in saline sandstone aquifers. 2nd International Forum on Recent
624 Developments of CCS Implementations. Athens, 26th-27th March.

625 Zevnik, L., Babic, M., Levec, J., 2006. Ultrasound speed and absorption study in near-critical CO_2: A
626 sensor for high-pressure application The Journal of Supercritical Fluids 36, 245-253.
627 http://dx.doi.org/10.1016/j.supflu.2005.06.003.

628 Zhang, J., 1996. Designing a cost effective and reliable pipeline leak detection system. Pipeline
629 Reliability Conference, Houston, USA, 19th-22th December.

630 Ziabakhsh-Ganji, Z., Kooi, H., 2014a. Sensitivity of Joule-Thomson cooling to impure CO_2 injection in
631 depleted gas reservoirs. Applied Energy 113, 434-451.
632 http://dx.doi.org/10.1016/j.apenergy.2013.07.059

633 Ziabakhsh-Ganji, Z., Kooi, H., 2014b. Sensitivity of the CO_2 storage capacity of underground
634 geological structures to the presence of SO_2 and other impurities. Applied Energy 135, 43-52.
635 http://dx.doi.org/10.1016/j.apenergy.2014.08.073.

636

Table

Table 1. Experimental speed of sound, c, in the CO_2+CH_3OH system at T = 263.15 K and at compositions x and pressures P.

P (MPa)	c (m s^{-1})	P (MPa)	c (m s^{-1})	P (MPa)	c (m s^{-1})	P (MPa)	c (m s^{-1})
$x_{CO_2} = 0.8005$							
6.00	715.0	35.20	931.9	64.83	1073.7	110.60	1235.7
9.77	752.1	39.99	958.0	70.01	1094.6	121.71	1269.0
14.79	795.6	44.89	983.3	75.05	1114.2	140.55	1321.7
20.11	836.3	50.00	1008.2	80.11	1133.2	158.97	1369.6
25.13	870.8	54.74	1030.1	90.13	1169.0	179.95	1419.9
29.95	901.1	60.08	1053.5	100.04	1202.2	196.30	1456.9
$x_{CO_2} = 0.9025$							
10.03	719.6	35.01	902.0	60.03	1026.1	89.88	1141.4
14.94	764.0	39.98	929.6	65.02	1047.3	99.98	1175.3
19.97	803.8	44.95	955.5	70.26	1068.7	109.60	1205.9
24.91	838.9	50.41	982.4	75.17	1087.8	120.18	1237.6
29.86	871.1	55.21	1004.7	80.08	1106.4		
$x_{CO_2} = 0.9503$							
3.80	633.5	24.92	829.4	54.91	995.6	110.06	1199.3
6.02	661.8	24.99	830.2	60.01	1018.3	119.96	1228.9
6.17	664.3	29.61	860.8	65.09	1039.8	140.00	1284.7
10.02	706.8	29.96	862.5	69.97	1059.9	159.90	1335.8
14.91	752.6	34.89	892.6	75.00	1079.5	179.99	1383.3
14.96	752.4	39.94	921.0	80.15	1098.9	194.49	1415.5
19.89	792.8	44.89	947.0	90.13	1134.4		
20.10	794.8	49.99	972.3	100.14	1168.0		
$x_{CO_2} = 0.9700$[a]							
3.28	626.2	24.92	829.4	60.01	1018.3	110.06	1199.3
3.80	633.5	29.96	862.5	65.09	1039.8	119.96	1228.9

5.05	649.7	34.89	892.6	69.97	1059.9	140.00	1284.7
6.02	661.8	39.94	921.0	75.00	1079.5	159.90	1335.8
10.02	706.8	44.89	947.0	80.15	1098.9	179.99	1383.3
14.96	752.4	49.99	972.3	90.13	1134.4	194.49	1415.5
19.89	792.8	54.91	995.6	100.14	1168.0		
			$x_{CO_2} = 0.9794$				
6.05	662.9	39.59	920.9	75.03	1081.7	160.48	1339.2
9.85	705.2	45.15	950.4	80.36	1101.8	160.48	1339.2
14.60	750.5	50.12	975.6	89.91	1135.9	180.44	1386.1
19.65	792.4	55.18	998.8	100.30	1170.8	195.38	1419.4
24.80	830.2	60.25	1021.4	110.19	1202.0		
29.76	863.1	65.97	1045.7	120.05	1231.5		
34.69	893.2	69.77	1061.1	139.56	1285.8		
			$x_{CO_2} = 0.9845$				
6.11	665.1	34.84	896.6	65.10	1044.7	110.11	1204.2
9.96	708.0	39.54	923.3	70.08	1064.9	120.77	1236.1
14.64	752.9	44.38	949.0	74.99	1084.3	139.56	1288.3
	793.3	50.19	978.0	79.96	1103.0	159.16	1338.3
24.71	831.8	54.91	1000.2	89.90	1138.5	179.47	1386.5
29.67	865.0	60.05	1023.2	100.07	1172.6		
			$x_{CO_2} = 0.9898$				
54.793	1003.4	75.44	1089.5	110.07	1207.6	179.81	1390.1
59.665	1025.2	80.43	1108.3	119.47	1235.7		
64.697	1046.6	90.23	1143.0	140.15	1293.1		
70.224	1069.3	101.20	1179.7	159.52	1342.3		

Standard uncertainties: $u_T = 0.015$ K, $u_P = 0.05$ MPa, $u_x = 2 \times 10^{-6}$, $u_c^* = 5.3 \times 10^{-4} c$, $u_c = 5.9 \times 10^{-4} c$.[a]

[a] Rivas et al. 2016.

Table 2. Experimental speed of sound, c, in the CO_2+CH_3OH system at T = 298.15 K and at compositions x and pressures P.

P (MPa)	c (m s^{-1})	P (MPa)	c (m s^{-1})	P (MPa)	c (m s^{-1})	P (MPa)	c (m s^{-1})
$x_{CO_2} = 0.8005$							
15.26	580.0	44.89	827.1	75.07	983.0	140.09	1212.0
19.71	629.3	49.68	855.5	80.14	1004.7	159.87	1267.4
24.87	679.9	55.49	888.8	90.51	1046.5	180.76	1321.2
29.92	722.8	60.31	913.7	99.98	1082.0		
34.98	761.4	65.06	937.3	109.95	1117.2		
39.97	795.8	70.08	960.7	120.21	1151.3		
$x_{CO_2} = 0.9025$							
14.96	550.1	39.82	772.5	65.00	915.0	109.67	1095.0
19.89	606.5	44.89	805.5	70.21	939.5	120.24	1130.1
24.84	654.9	50.08	836.4	75.28	962.3	139.48	1189.0
29.89	698.4	55.06	864.3	90.39	1024.8		
34.85	737.1	60.11	890.7	99.92	1060.7		
$x_{CO_2} = 0.9503$							
15.04	534.4	50.12	831.3	75.27	957.5	120.16	1124.7
24.90	647.1	55.04	858.9	80.29	979.0	140.53	1186.9
34.90	731.4	59.70	883.6	90.09	1018.7	159.68	1240.0
39.97	767.8	65.14	910.6	99.88	1055.4	178.78	1288.7
44.93	800.1	70.32	935.3	109.68	1090.1		
$x_{CO_2} = 0.9700$							
20.04	597.6	44.84	802.7	74.99	959.8	110.38	1096.0
24.95	649.5	50.47	836.5	80.32	982.7	120.07	1127.8
29.89	694.4	54.96	861.8	81.42	987.4	140.10	1188.7
34.82	733.7	59.78	887.3	90.50	1023.8	160.14	1244.0
39.83	769.8	64.96	913.4	99.58	1057.9	170.64	1271.3

39.88	770.1	70.20	938.2	109.40	1092.6		
$x_{CO_2} = 0.9794$							
29.87	696.2	54.88	863.6	79.93	983.2	140.07	1190.5
34.92	736.5	60.22	891.9	90.55	1026.1	159.98	1245.5
39.97	772.8	65.26	917.0	100.14	1062.0		
44.94	805.4	70.33	940.9	109.99	1096.5		
50.18	837.1	75.17	962.8	120.19	1130.2		
$x_{CO_2} = 0.9845$							
44.80	806.6	70.39	943.1	119.43	1129.2	179.95	1297.2
50.19	839.2	80.03	985.5	139.95	1191.4		
59.91	892.2	100.60	1065.3	159.48	1245.3		
$x_{CO_2} = 0.9898$							
59.98	892.6	79.93	985.0	120.25	1131.6	160.32	1247.2
65.33	919.3	89.96	1025.5	130.39	1163.1	170.19	1272.8
70.30	942.7	100.24	1063.9	140.04	1191.4		
75.33	965.3	110.18	1098.7	149.87	1219.3		

Standard uncertainties: $u_T = 0.015$ K, $u_P = 0.05$ MPa, $u_x = 2 \times 10^{-6}$, $u_c^* = 5.3 \times 10^{-4} c$, $u_c = 5.9 \times 10^{-4} c$.[a]

[a] Rivas et al. 2016.

Table 3. Experimental speed of sound, c, in the CO_2+CH_3OH system at T = 323.15 K and at compositions x and pressures P.

P (MPa)	c (m s^{-1})	P (MPa)	c (m s^{-1})	P (MPa)	c (m s^{-1})	P (MPa)	c (m s^{-1})
$x_{CO_2} = 0.8005$							
24.98	558.1	60.39	832.9	80.33	932.0	120.47	1087.8
30.07	612.5	65.08	858.2	90.06	973.9	140.70	1152.8
50.04	771.9	70.16	884.0	99.72	1012.7	159.50	1207.7
55.40	804.7	75.36	909.1	110.02	1051.2	180.28	1263.6
$x_{CO_2} = 0.9025$							
24.90	538.9	50.13	750.6	80.16	910.5	140.17	1130.4
29.95	593.0	54.95	780.5	90.12	953.7	160.42	1189.3
34.91	638.4	59.87	808.9	99.79	992.4		
39.98	679.6	65.02	836.9	110.29	1031.6		
45.08	716.9	74.85	885.9	120.09	1065.9		
$x_{CO_2} = 0.9503$							
29.99	589.1	50.01	747.2	69.99	860.3	99.49	989.2
34.91	634.9	55.08	778.9	75.12	885.2	110.19	1029.1
40.04	676.9	59.73	805.8	79.95	907.6	120.29	1064.4
45.00	713.4	64.87	833.9	89.27	948.2	140.61	1129.3
$x_{CO_2} = 0.9700$							
40.00	680.0	64.94	836.9	89.99	953.5	140.13	1129.4
44.88	715.2	70.03	863.0	100.09	993.8	159.98	1186.6
50.07	750.3	74.97	887.0	109.98	1030.5	171.27	1217.0
60.02	810.1	80.16	911.0	120.04	1065.4		
$x_{CO_2} = 0.9794$							
54.47	777.7	70.33	864.4	90.57	955.8	119.81	1064.4
60.08	810.4	75.03	887.4	100.13	993.8	139.42	1127.3
65.26	838.5	80.29	911.5	109.91	1030.0	159.41	1184.4

$x_{CO_2} = 0.9845$							
69.67	860.4	89.68	951.3	120.42	1065.6	150.01	1157.4
75.24	887.4	100.05	992.7	130.13	1097.3	159.54	1184.2
80.28	910.7	110.20	1030.2	140.84	1130.4		
$x_{CO_2} = 0.9898$							
95.03	971.9	109.51	1026.6	129.94	1095.6	150.71	1158.2
99.68	990.1	119.49	1061.4	139.88	1126.3		

Standard uncertainties: $u_T = 0.015$ K, $u_P = 0.05$ MPa, $u_x = 2 \times 10^{-6}$, $u_c^* = 5.3 \times 10^{-4} c$, $u_c = 5.9 \times 10^{-4} c$.[a]

[a] Rivas et al. 2016.

Table 4. Coefficients of equation 7 and the mean relative deviations for the CO_2+CH_3OH mixtures at compositions x and temperatures T.

x_{CO_2}	T (K)	$10 \times a_1$ (MPa m^{-1} s)	$10^4 \times a_2$ (MPa m^{-2} s^2)	$10^8 \times a_3$ (MPa m^{-3} s^3)	MRD_c (%)
0.8005	263.15	2.51877	2.4355	6.345	0.007
	298.15	2.17429	2.2126	7.287	0.033
	323.15	2.00343	2.1208	6.700	0.042
0.9025	263.15	2.50605	2.5074	7.390	0.004
	298.15	2.16483	2.2431	8.072	0.031
	323.15	2.00504	2.1074	6.754	0.005
0.9503	263.15	2.50388	2.5430	7.332	0.019
	298.15	2.16489	2.2715	7.399	0.012
	323.15	2.00015	2.1274	7.100	0.004
0.9700	263.15[a]	2.50355	2.5400	7.258	0.012
	298.15	2.16314	2.2930	7.535	0.008
	323.15	2.00467	2.1435	7.613	0.009
0.9794	263.15	2.50071	2.5495	7.483	0.009
	298.15	2.16464	2.2995	7.558	0.004
	323.15	2.00334	2.1419	8.354	0.010
0.9845	263.15	2.50066	2.556	7.533	0.008
	298.15	2.16900	2.3230	7.377	0.003
	323.15	2.00545	2.1602	7.498	0.001
0.9898	263.15	2.50598	2.5363	8.680	0.004
	298.15	2.16843	2.3351	7.289	0.006
	323.15	2.06645	1.8687	12.67	0.003
Overall mean relative deviation: $\overline{MRD_c}$=0.012%.					

$MRD_c(\%) = \frac{100}{N}\sum_i^N \left|\frac{c_i - c_{i,fit}}{c_i}\right|$; $\overline{MRD_c}(\%) = \frac{100}{N'}\sum_{i=1}^{N'} \left|\frac{c_i - c_{i,fit}}{c_i}\right|$. c_i: experimental datum; $c_{i,fit}$: value obtained for the property at the same state point from the correlating equation 7; N: number of points for each isopleth and isotherm; N': total number of points.

[a]Rivas et al. 2016.

Table 5. Experimental speed of sound, c, in the CO_2+SO_2 mixture with $x_{CO_2} = 0.8969$ and $x_{SO_2} = 0.1031$ at temperatures T and pressures P.

P (MPa)	c (m s^{-1})	P (MPa)	c (m s^{-1})	P (MPa)	c (m s^{-1})	P (MPa)	c (m s^{-1})
$T = 263.15$ K							
7.99	763.3	30.00	915.7	55.00	1037.4	80.00	1132.9
9.99	780.2	35.00	943.1	60.00	1059.4	85.00	1149.9
14.99	820.2	40.00	968.8	65.00	1078.0	90.00	1166.5
20.00	855.5	45.00	992.8	70.00	1096.9	95.00	1182.4
25.00	886.2	50.00	1015.6	75.00	1115.2		
$T = 273.15$ K							
17.99	785.1	40.00	923.2	65.00	1038.9	90.00	1131.3
19.99	800.5	45.00	949.1	70.00	1058.8	95.00	1147.9
25.00	836.0	50.00	973.3	75.00	1078.0	99.99	1163.8
30.00	866.0	55.00	996.2	80.00	1096.4		
34.99	895.6	60.00	1018.1	85.00	1114.2		
$T = 293.15$ K							
31.03	778.4	55.00	917.5	80.00	1026.9	105.00	1116.1
34.99	805.5	60.01	941.6	85.00	1046.0	110.00	1132.3
39.98	837.6	65.00	964.4	90.00	1064.5	115.01	1148.0
44.99	866.2	70.00	986.2	95.00	1082.2		
49.99	893.3	75.00	1007.0	100.00	1099.4		
$T = 304.16$ K							
45.97	828.7	65.03	925.9	90.00	1029.8	115.01	1115.9
50.00	851.7	69.99	950.5	95.00	1048.3	119.99	1131.8
55.00	878.6	75.00	972.1	100.00	1066.1		
59.98	903.8	79.99	990.9	105.00	1083.3		
65.00	927.7	85.00	1010.7	110.00	1099.9		
$T = 313.15$ K							

62.01	882.4	79.99	962.9	100.00	1039.8	120.00	1107.1
64.99	897.1	84.99	983.3	105.00	1057.5	124.99	1122.5
69.99	920.5	90.00	1002.8	110.00	1074.5		
74.99	943.1	95.00	1021.7	115.00	1091.0		
$T = 333.15$ K							
80.99	909.6	105.00	1003.7	120.00	1055.4	132.49	1095.1
85.00	926.8	110.00	1021.4	122.50	1063.6	135.00	1102.9
90.00	947.5	112.51	1030.1	125.00	1071.7		
94.99	967.5	115.00	1040.0	127.50	1079.6		
99.99	986.5	117.50	1047.1	130.00	1087.5		
$T = 353.15$ K							
97.99	929.4	113.99	988.7	127.99	1036.3	138.00	1066.7
100.00	936.7	116.00	995.8	129.98	1041.4	140.00	1072.7
101.97	944.4	118.00	1002.7	132.00	1049.1	142.01	1078.9
103.99	952.1	120.00	1009.5	132.49	1049.4	144.00	1084.8
106.01	959.7	122.00	1016.3	133.97	1054.0	145.01	1087.2
108.00	967.1	124.00	1023.0	134.96	1057.3		
109.98	974.3	126.00	1028.4	136.01	1060.4		
111.99	981.6	127.48	1033.3	137.49	1065.0		
$T = 373.19$ K							
112.49	940.4	125.00	984.6	135.00	1017.7	144.00	1044.3
115.00	949.7	127.51	993.1	135.99	1019.3	145.99	1050.4
117.50	958.5	129.99	1001.3	138.00	1027.1	148.00	1056.4
119.99	967.3	132.49	1009.6	140.00	1032.0	150.00	1062.3
122.50	976.1	133.98	1012.9	141.98	1038.1		

Standard uncertainties: $u_T = 0.015$ K, $u_P = 0.05$ MPa, $u_x = 1 \times 10^{-6}$, $u_c^* = 6.2 \times 10^{-4} c$, $u_c = 6.2 \times 10^{-4} c$.

Table 6. Experimental speed of sound, c, in the CO_2+CH_3OH+SO_2 mixture with $x_{CO_2} = 0.8889$, $x_{CH_3OH} = 0.0080$ and $x_{SO_2} = 0.1031$ at temperatures T and pressures P.

P (MPa)	c (m s^{-1})	P (MPa)	c (m s^{-1})	P (MPa)	c (m s^{-1})	P (MPa)	c (m s^{-1})
$T = 263.15$ K							
8.00	754.8	39.98	965.8	74.98	1113.2	140.00	1308.4
9.99	772.9	44.97	990.0	79.95	1131.1	149.97	1333.0
14.99	813.7	49.97	1013.0	89.98	1164.8	160.00	1357.0
19.95	849.5	54.96	1034.8	99.98	1196.7	170.03	1379.9
24.97	882.2	59.98	1055.8	110.00	1226.7	180.03	1402.2
29.97	912.0	65.00	1075.7	119.96	1255.1	190.00	1423.4
35.01	939.9	69.99	1094.9	129.97	1282.3		
$T = 273.15$ K							
17.97	777.7	49.96	970.7	84.98	1112.3	140.00	1278.1
20.01	794.0	54.97	993.9	89.98	1130.1	149.92	1303.1
24.95	829.6	59.98	1015.9	99.98	1162.5	160.00	1328.2
30.00	862.7	64.97	1036.8	109.95	1193.8	169.96	1351.6
34.97	892.4	70.01	1056.8	114.99	1208.5	179.99	1374.5
40.02	919.4	74.95	1076.2	119.97	1223.4	189.95	1396.0
45.00	946.6	79.98	1094.8	129.98	1251.0		
$T = 293.15$ K							
34.98	801.0	64.98	962.8	110.01	1131.8	169.97	1297.5
40.00	833.1	69.99	984.7	119.98	1162.8	180.01	1321.2
45.00	862.6	75.01	1005.7	129.96	1192.3	189.99	1344.0
49.97	889.8	79.97	1025.9	139.96	1220.3		
54.96	915.4	89.99	1063.8	149.99	1247.2		
59.98	939.7	100.00	1098.8	159.97	1272.8		
$T = 304.16$ K							
47.06	830.9	70.00	947.0	109.98	1099.2	159.99	1244.1

50.02	847.3	74.99	968.8	119.98	1131.2	169.98	1269.2
54.98	874.5	79.95	989.4	130.01	1161.6	179.99	1293.6
59.99	900.0	89.99	1028.9	139.99	1190.2	189.99	1316.8
65.00	924.0	100.01	1065.4	150.00	1217.6		
$T = 313.15$ K							
54.92	843.3	79.99	961.6	129.97	1137.4	179.98	1271.7
60.01	869.2	89.95	1001.5	139.99	1166.8	189.98	1295.2
65.04	894.2	99.96	1039.0	149.93	1194.2		
69.98	917.9	109.95	1073.8	159.94	1221.2		
75.00	940.3	120.01	1106.7	169.95	1247.1		
$T = 333.15$ K							
69.98	856.2	100.03	984.9	140.02	1117.6	180.01	1226.2
74.94	880.1	110.04	1021.0	149.98	1146.6	189.97	1250.5
79.99	903.0	119.96	1055.0	159.99	1174.4		
89.98	945.3	130.00	1087.3	169.96	1200.7		
$T = 353.15$ K							
84.98	872.7	109.97	972.8	134.99	1057.4	170.00	1158.2
90.00	894.4	115.00	991.0	139.97	1072.6	179.93	1184.1
95.00	915.1	119.99	1008.1	144.96	1087.8	190.10	1209.3
100.00	935.1	124.97	1025.0	149.96	1102.5		
105.00	954.3	130.00	1041.3	160.01	1131.0		
$T = 373.19$ K							
99.99	890.5	119.98	965.4	139.95	1031.6	169.95	1119.1
104.96	910.2	124.96	982.7	145.02	1047.2	179.93	1145.5
110.01	929.3	129.96	999.5	150.00	1062.2	189.94	1171.2
115.04	947.7	134.96	1015.9	159.93	1091.2		

Standard uncertainties: $u_T = 0.015$ K, $u_P = 0.05$ MPa, $u_x = 2 \times 10^{-6}$, $u_c^* = 8.1 \times 10^{-4} c$, $u_c = 8.1 \times 10^{-4} c$.

Table 7. Coefficients and $P^{\#}$of equation 7 along with the mean relative deviations for the CO_2+SO_2 mixture with $x_{CO_2} = 0.8969$ and $x_{SO_2} = 0.1031$ at temperatures T.

T (K)	$P^{\#}$ (MPa)	$10 \times a_1$ (MPa m^{-1} s)	$10^4 \times a_2$ (MPa m^{-2} s^2)	$10^8 \times a_3$ (MPa m^{-3} s^3)	MRD_c (%)
263.15	30.00	1.76485	2.2533	10.30	0.030
273.15	30.00	1.64259	2.0347	11.88	0.019
293.15	50.00	1.92170	2.3548	4.024	0.025
304.16	65.00	2.17783	2.5527	-1.847	0.027
313.15	80.00	2.42432	2.3997	6.009	0.020
333.15	100.00	2.70016	2.6889	-1.251	0.022
353.15	110.00	2.78887	2.7460	14.29	0.027
373.19	120.00	2.86153	3.7143	-51.84	0.030
Overall mean relative deviation $\overline{MRD_c}$=0.025%.					

$MRD_c(\%) = \frac{100}{N}\sum_i^N \left|\frac{c_i - c_{i,fit}}{c_i}\right|$; $\overline{MRD_c}(\%) = \frac{100}{N'}\sum_{i=1}^{N'} \left|\frac{c_i - c_{i,fit}}{c_i}\right|$. c_i: experimental datum; $c_{i,fit}$: value obtained for the property at the same state point from the correlating equation 7; N: number of points for each isotherm; N': total number of points.

Table 8. Coefficients and $P^{\#}$of equation 7 along with the mean relative deviations for the CO_2+CH_3OH+SO_2 mixture with $x_{CO_2} = 0.8889$, $x_{CH_3OH} = 0.0080$ and $x_{SO_2} = 0.1031$ at temperatures T.

T (K)	$P^{\#}$ (MPa)	$10 \times a_1$ (MPa m^{-1} s)	$10^4 \times a_2$ (MPa m^{-2} s^2)	$10^8 \times a_3$ (MPa m^{-3} s^3)	MRD_c (%)
263.15	50.00	2.22847	2.5432	8.303	0.009
273.15	50.00	2.10376	2.4528	7.911	0.017
293.15	80.00	2.54506	2.5949	8.365	0.006
304.16	90.00	2.65293	2.6121	8.018	0.008
313.15	95.00	2.68592	2.5895	8.536	0.015
333.15	100.00	2.65349	2.5408	7.572	0.007
353.15	120.00	2.92232	2.6115	8.911	0.005
373.19	125.00	2.93618	2.5359	9.762	0.006
Overall mean relative deviation $\overline{MRD_c}$=0.010%.					

$MRD_c(\%) = \frac{100}{N}\sum_i^N \left|\frac{c_i - c_{i,fit}}{c_i}\right|$; $\overline{MRD_c}(\%) = \frac{100}{N'}\sum_{i=1}^{N'} \left|\frac{c_i - c_{i,fit}}{c_i}\right|$. c_i: experimental datum; $c_{i,fit}$: value obtained for the property at the same state point from the correlating equation 7; N: number of points for each isotherm; N': total number of points.

Table 9. Speed of sound in the CO_2+CH_3OH mixtures calculated using equation (7), c_{fit}, and the coefficients of equation (8), c_i, at temperatures T and at pressures P. c_0 is the derived speed of sound in pure CO_2, and $u_r(c_0)$ is the standard relative uncertainty of c_0. Italicized figures are extrapolated values.

T (K)	P (MPa)	c_{fit} (m s^{-1}) x_{CO_2}=					c_0 (m s^{-1})	c_1 (m s^{-1})	c_2 (m s^{-1})	$u_r(c_0)$ (%)
		0.9503	0.9700[a]	0.9794	0.9845	0.9898				
263.15	8	684.93	684.73	685.50	687.00		691.61	-387	5087	0.24
	10	706.15	705.96	706.87	708.57		713.82	-440	5753	0.25
	15	753.13	752.97	754.14	756.18		762.63	-538	6985	0.26
	25	830.13	829.98	831.53	833.92		841.81	-654	8437	0.25
	35	893.30	893.16	894.95	897.51	*902.28*	910.43	-994	13118	0.08
	50	972.48	972.34	974.35	977.02	*980.95*	988.79	-927	12092	0.16
	60	1018.25	1018.11	1020.21	1022.90	1026.61	1034.38	-911	11826	0.13
	70	1059.93	1059.80	1061.95	1064.65	1068.24	1075.98	-902	11679	0.12
	75	1079.51	1079.38	1081.55	1084.25	1087.80	1095.53	-899	11626	0.12
	80	1098.35	1098.23	1100.41	1103.11	1106.63	1114.35	-896	11578	0.12
	100	1167.60	1167.50	1169.70	1172.37	1175.81	1183.43	-883	11383	0.11
	120	1229.13	1229.05	1231.23	1233.84	1237.20	1244.67	-864	11118	0.10
	125	1243.54	1243.47	1245.63	1248.24	1251.57	1258.99	-858	11038	0.10
	140	1284.81	1284.76	1286.88	1289.44	1292.67	1299.93	-838	10762	0.10
	150	1310.86	1310.83	1312.92	1315.45	1318.60	1325.73	-823	10550	0.10
	160	1335.88	1335.87	1337.91	1340.42	1343.48	1350.47	-805	10318	0.10
	175	1371.69	1371.70	1373.69	1376.15	1379.06	1385.82	-777	9935	0.10
	180	1383.21	1383.23	1385.19	1387.64	1390.49	1397.18	-767	9799	0.09
	200	*1427.43*	*1427.48*	*1429.35*	*1431.73*	*1434.35*	1440.69	-724	9216	0.09
298.15	25	648.39	650.03	*652.10*	*652.94*		657.66	-346	3214	0.19
	35	732.30	734.96	737.12	*738.89*	*738.29*	740.74	-183	219	0.27
	50	830.58	833.85	836.02	838.07	*837.87*	840.73	-236	619	0.21
	60	885.13	888.56	890.71	892.73	892.62	895.42	-234	512	0.19

	70	933.76	937.26	939.38	941.32	941.24	943.92	-222	330	0.18
	75	956.32	959.83	961.93	963.83	963.75	966.35	-215	230	0.17
	80	977.88	981.39	983.48	985.32	985.24	987.77	-207	130	0.16
	100	1056.03	1059.48	1061.49	1063.13	1063.01	1065.23	-175	-238	0.15
	120	1124.27	1127.60	1129.55	1130.99	1130.83	1132.76	-146	-528	0.14
	125	1140.13	1143.42	1145.35	1146.75	1146.57	1148.45	-139	-587	0.13
	140	1185.28	1188.45	1190.34	1191.62	1191.40	1193.11	-122	-738	0.13
	150	1213.62	1216.71	1218.56	1219.77	1219.53	1221.14	-112	-817	0.13
	160	1240.73	1243.73	1245.55	1246.70	1246.43	1247.95	-103	-880	0.12
	175	1279.35	*1282.22*	*1284.00*	1285.06	*1284.76*	1286.17	-91	-948	0.12
	180	1291.73	*1294.56*	*1296.32*	1297.35	*1297.05*	1298.42	-88	-964	0.12
	200	*1339.10*	*1341.75*	*1343.46*	*1344.39*	*1344.05*	1345.31	-77	-1002	0.12
323.15	50	747.17	749.99	*749.95*	*749.08*		745.36	341	-6138	0.14
	60	807.33	810.01	809.96	*809.20*		805.73	317	-5739	0.12
	70	860.25	862.82	862.80	862.01	*862.45*	860.77	170	-3615	0.14
	75	884.61	887.12	887.12	886.30	*886.13*	884.01	308	-4557	0.11
	80	907.80	910.26	910.26	909.41	*908.84*	906.41	285	-5180	0.08
	100	991.20	993.39	993.39	992.45	991.30	988.44	350	-5935	0.10
	120	1063.37	1065.26	1065.15	1064.20	1063.07	1060.24	343	-5649	0.09
	125	1080.07	1081.88	1081.72	1080.79	1079.66	1076.85	340	-5547	0.09
	140	1127.49	1129.05	1128.75	1127.89	1126.72	1123.96	333	-5287	0.09
	150	*1157.16*	1158.55	1158.14	1157.34	1156.09	1153.32	334	-5181	0.09
	160	*1185.49*	1186.70	1186.16	1185.45	*1184.06*	1181.25	341	-5147	0.09
	175	*1225.77*	*1226.71*	*1225.95*	*1225.40*	*1223.68*	1220.75	361	-5235	0.10
	180	*1238.66*	*1239.51*	*1238.68*	*1238.19*	*1236.32*	1233.34	370	-5301	0.10
	200	*1287.91*	*1288.39*	*1287.23*	*1287.00*	*1284.45*	1281.15	420	-5745	0.13

Overall standard relative uncertainty of c_0, $\overline{u_r(c_0)}$=0.12%.

Standard uncertainty of *c*: $u_c = 5.9 \times 10^{-4} c$ [b]. $\overline{u_r(c_0)} = \frac{1}{N}\sum_i^N u_r(c_0)_i$; N: number of pressures in Table 9.

[a]At 263.15 K, experimental data from Rivas et al. 2016. [b]Rivas et al. 2016.

Table 10. Comparison between the experimental $P-c-T-x_{\mathrm{CO_2}}$ data for the $\mathrm{CO_2}$+$\mathrm{CH_3OH}$ mixtures studied in this work and those calculated using the PC-SAFT EoS and the REFPROP 9 software, at temperatures T.

	MRD_c (%) $T = 263.15$ K		MRD_c (%) $T = 298.15$ K		MRD_c (%) $T = 323.15$ K	
$x_{\mathrm{CO_2}}$	PC-SAFT	REFPROP 9	PC-SAFT	REFPROP 9	PC-SAFT	REFPROP 9
0.8005	2.12	11.7	2.09	12.9	2.16	11.0
0.9025	2.56	7.12	1.60	7.65	1.57	6.49
0.9503	2.82	4.95	2.05	4.23	1.55	3.16
0.9700	3.08	3.62	2.61	2.29	2.56	1.40
0.9794	3.98	2.15	3.22	1.34	2.95	0.86
0.9845	4.32	1.55	3.66	0.85	3.09	0.74
0.9898	5.01	0.80	3.86	0.64	3.15	0.65
Overall mean relative deviations $\overline{MRD_c} = 2.83\%$ for PC-SAFT and 4.97% for GERG						

$MRD_c(\%) = \frac{100}{N}\sum_{i=1}^{N}\left|\frac{c_{i.\mathrm{model}}-c_{i.\mathrm{exp}}}{c_{i.\mathrm{exp}}}\right|$; $\overline{MRD_c}(\%) = \frac{100}{N'}\sum_{i=1}^{N'}\left|\frac{c_{i.\mathrm{model}}-c_{i.\mathrm{exp}}}{c_{i.\mathrm{exp}}}\right|$. $c_{i.\mathrm{exp}}$: experimental values; $c_{i.\mathrm{model}}$: values calculated using the PC-SAFT EoS or the REFPROP 9 software; N: number of points for each isotherm and isopleth; N': total number of points.

Table 11. Comparison between the experimental $P-c-T$ data for the CO_2+SO_2 ($x_{CO_2}=0.8969, x_{SO_2}=0.1031$) and CO_2+CH_3OH+SO_2 ($x_{CO_2}=0.8889$, $x_{CH_3OH}=0.0080$, $x_{SO_2}=0.1031$) mixtures studied in this work and those calculated using the PC-SAFT EoS and the REFPROP 9 software at temperatures T. The ternary mixture was modeled as a ternary (a) and binary mixture of composition $x_{CO_2}=0.8969$, $x_{SO_2}=0.1031$ (b).

	MRD_c (%) CO_2+SO_2		MRD_c (%) CO_2+CH_3OH+SO_2(a)		MRD_c (%) CO_2+CH_3OH+SO_2(b)	
T (K)	PC-SAFT	REFPROP 9	PC-SAFT	REFPROP 9	PC-SAFT	REFPROP 9
263.15	2.52	3.19	4.32	2.16	2.83	1.86
273.15	2.32	2.51	4.04	1.66	2.66	1.44
293.15	2.14	1.43	3.49	1.14	2.36	1.02
304.16	2.23	0.92	3.20	0.89	2.29	0.84
313.15	2.28	0.53	3.00	0.75	2.27	0.79
333.15	2.20	0.53	2.55	0.70	2.12	0.96
353.15	2.04	0.87	2.16	0.96	1.94	1.25
373.19	1.88	1.12	1.77	1.23	1.76	1.51
$\overline{MRD_c}$ (%)	2.19	1.39	3.24	1.28	2.35	1.26

$MRD_c(\%)=\frac{100}{N}\sum_{i=1}^{N}\left|\frac{c_{i.\mathrm{model}}-c_{i.\mathrm{exp}}}{c_{i.\mathrm{exp}}}\right|$; $\overline{MRD_c}(\%)=\frac{100}{N'}\sum_{i=1}^{N'}\left|\frac{c_{i.\mathrm{model}}-c_{i.\mathrm{exp}}}{c_{i.\mathrm{exp}}}\right|$. $c_{i.\mathrm{exp}}$: experimental values; $c_{i.\mathrm{model}}$: values calculated using the PC-SAFT EoS or the REFPROP 9 software; N: number of points for each mixture and isotherm; N': total number of points for each mixture.

Figure

Figure 1. Speed of sound, c, in CO_2+CH_3OH with $x_{CO_2} = 0.9503$ at temperatures T and pressures P. Symbols, experimental points: ■, T = 263.15 K; ▲, T = 298.15 K; ★, T = 323.15 K. Solid lines, PC-SAFT EoS; dashed lines, REFPROP 9 software.

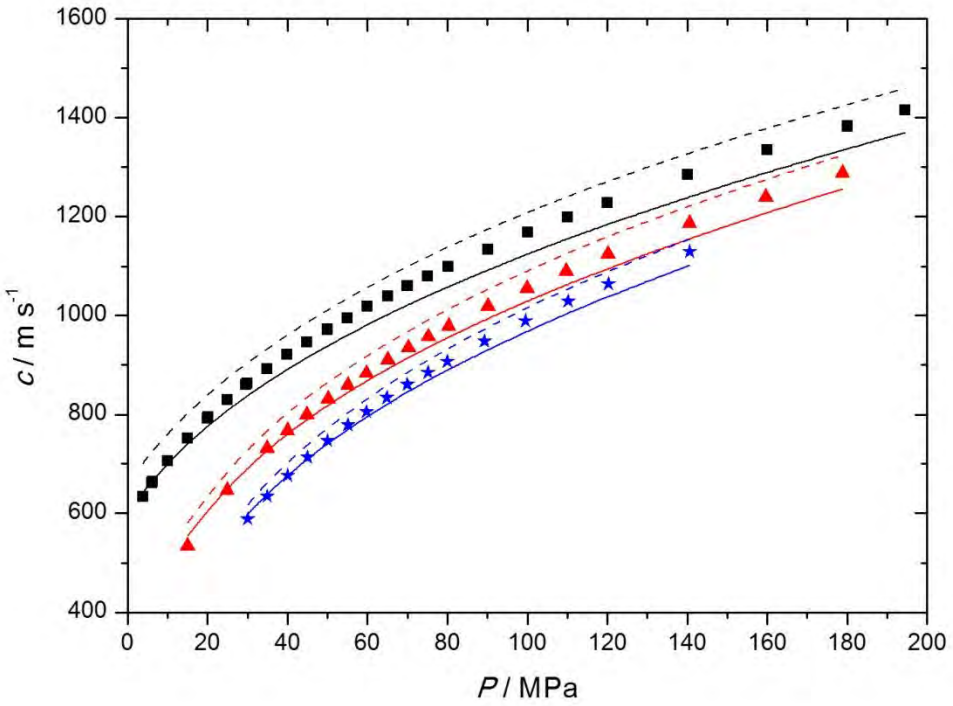

Figure 2. Relative deviations of the experimental speed of sound, c, from the values obtained from equation (7), c_{fit}, for all experimental points of the studied CO_2+CH_3OH mixtures. ■, T = 263.15 K; ▲, T = 298.15 K; ★, T = 323.15 K. The deviations of the data used in the section 5.1 range between -0.05% and +0.08% (dotted lines).

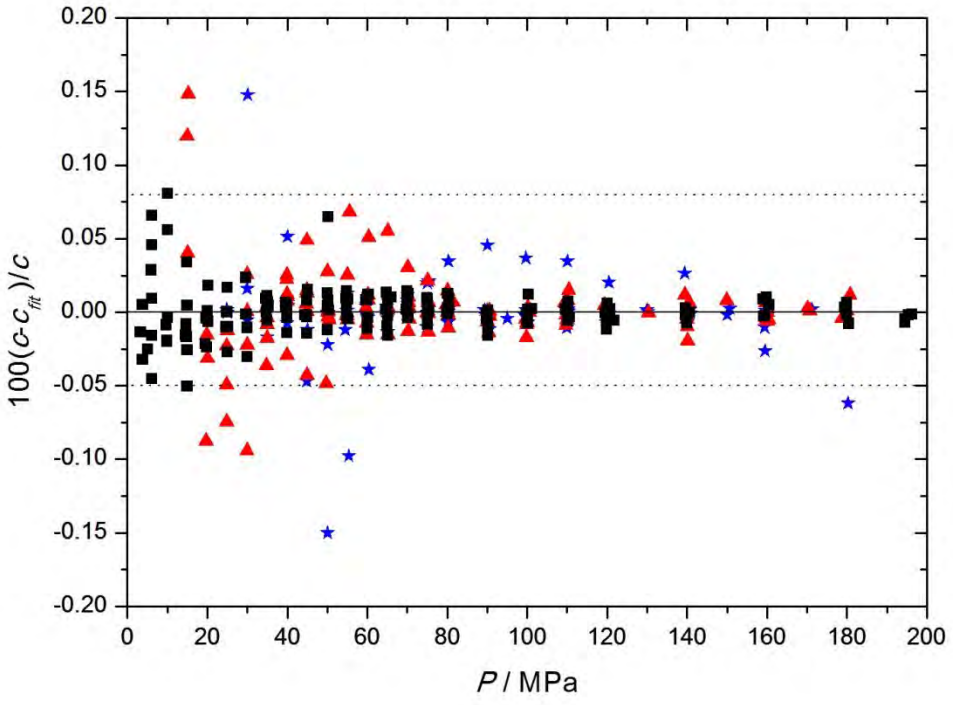

Figure 3. Speed of sound, c, in CO_2+SO_2 with $x_{CO_2} = 0.8969$ and $x_{SO_2} = 0.1031$ at temperatures T and pressures P. Symbols, experimental points: ■, T = 263.15 K; ▲, T = 293.15 K; ▼, T = 333.15 K; ★, T = 373.19 K. Solid lines, PC-SAFT EoS; dashed lines, REFPROP 9 software.

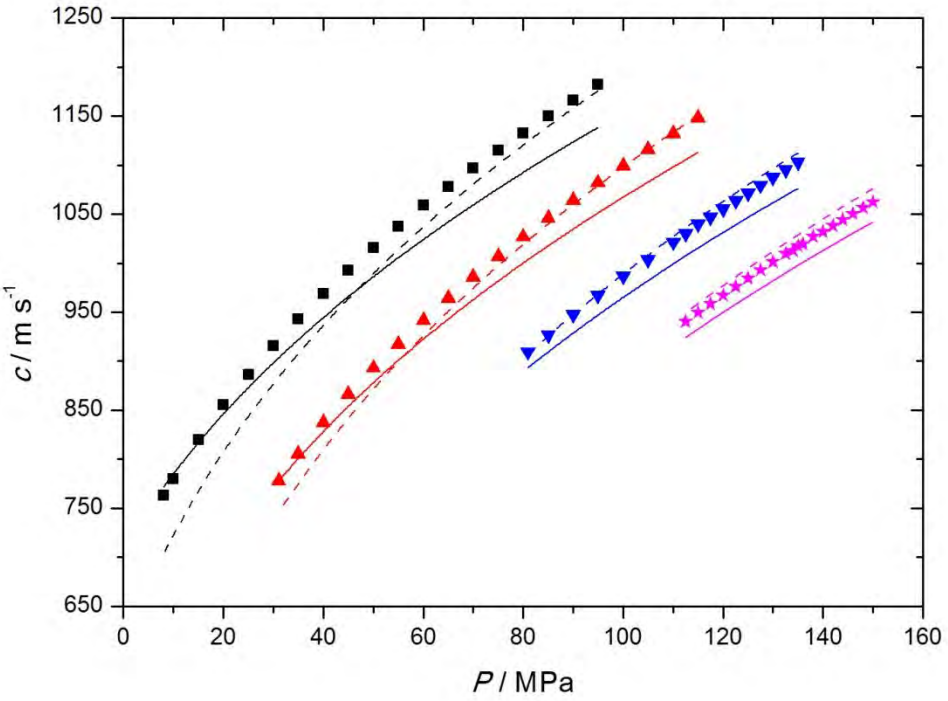

Figure 4. Speed of sound, c, in CO_2+CH_3OH+SO_2 with $x_{CO_2} = 0.8889$, $x_{CH_3OH} = 0.0080$ and $x_{SO_2} = 0.1031$ at temperatures T and pressures P. Symbols, experimental points: ■, T = 263.15 K; ▲, T = 293.15 K; ▼, T = 333.15 K; ★, T = 373.19 K. Solid lines, PC-SAFT EoS; dashed lines, REFPROP 9 software; system modeled as a binary mixture with $x_{CO_2} = 0.8989$, $x_{SO_2} = 0.1031$.

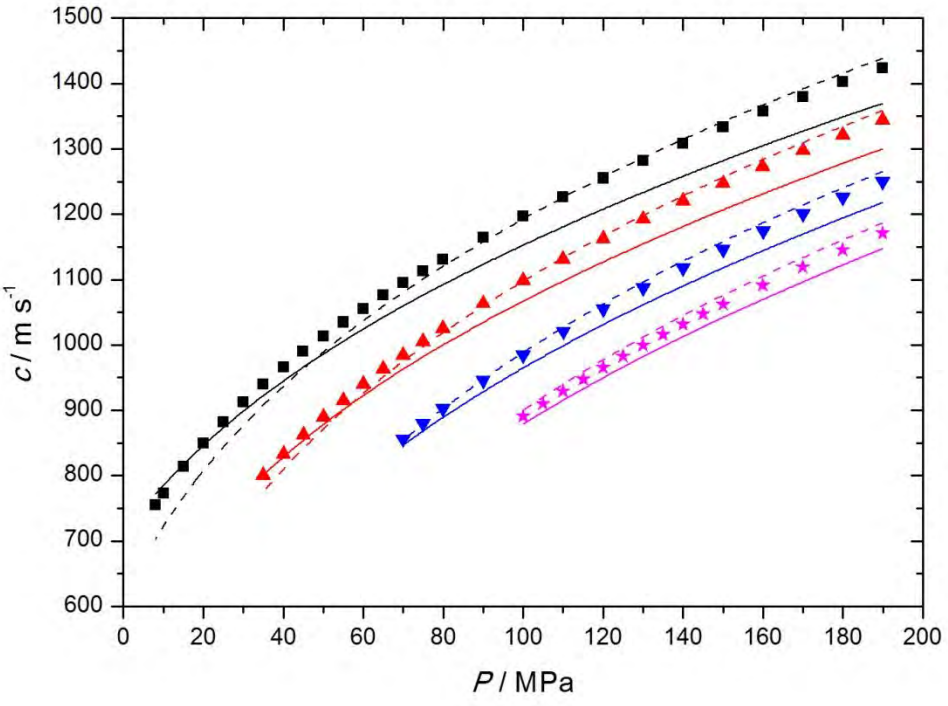

Figure 5. Speed of sound, c, in pure CO_2 versus pressure, P, at temperatures T. ■, T = 263.15 K; ▲, T = 298.15 K; ★, T = 323.15 K.

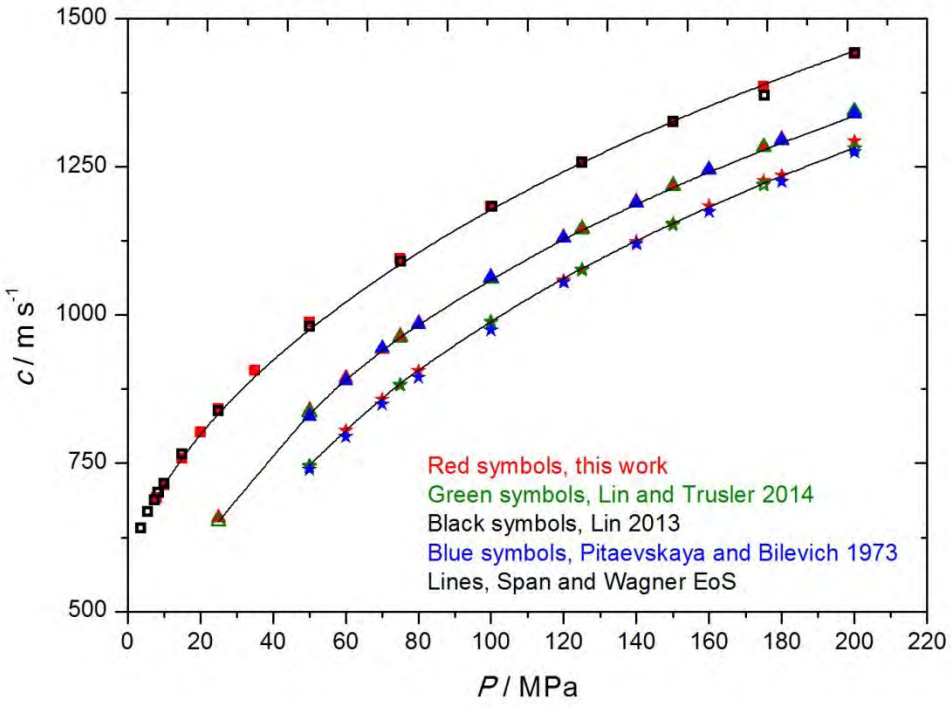

Figure 6. Speed of sound, c, in pure CO_2 versus temperature, T, at pressures P. ■, P = 8 MPa; □ , P = 15 MPa; ●, P = 25 MPa; ▲, P = 50 MPa; △ , P = 75 MPa; ▼, P = 100 MPa; ▽, P = 125 MPa; ◆, P = 150 MPa; ◇, P = 175 MPa; ★, P = 200 MPa.

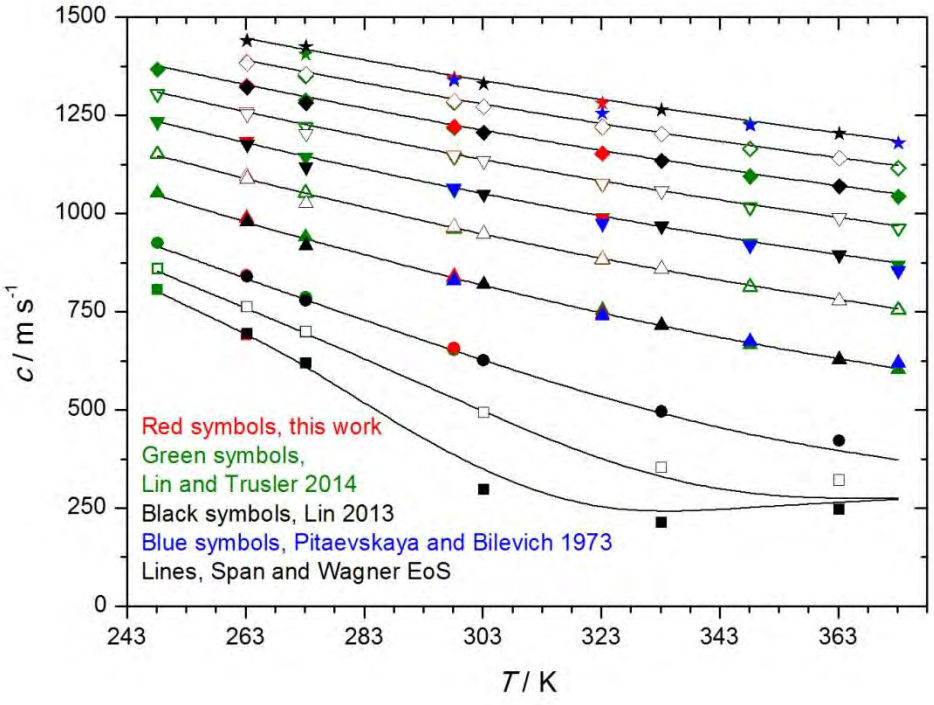

Figure 7. Relative deviations of the speed of sound in pure CO_2 obtained in this work and those in the literature, c, from the values obtained using the Span and Wagner EoS, c_{EoS}. ■, T = 263.15 K; ▲, T = 298.15 K; ★, T = 323.15 K.

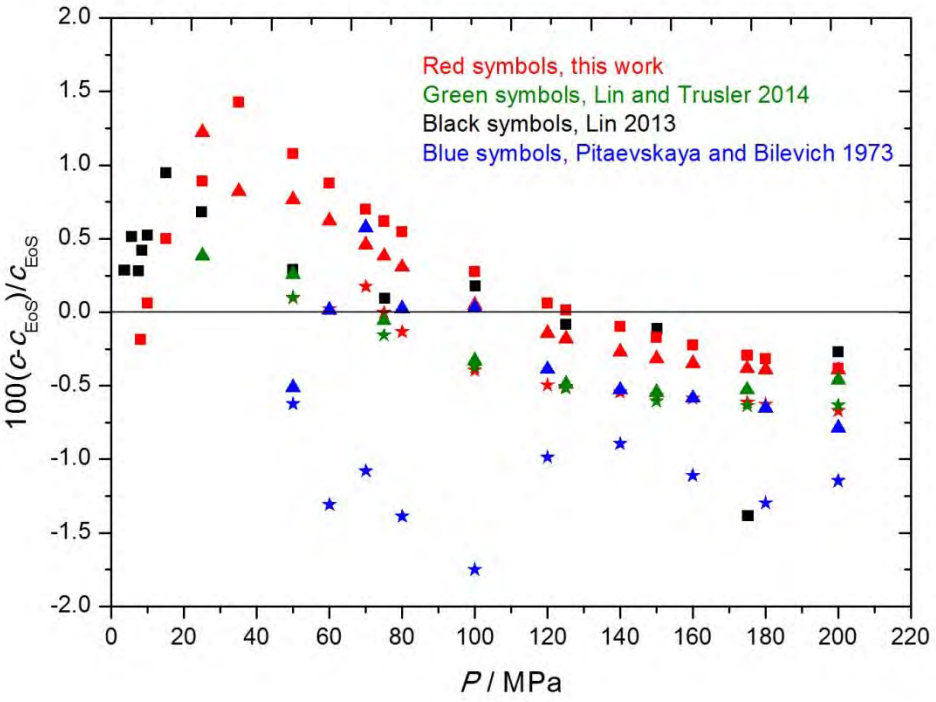

Figure 8. Relative deviations of the experimental speed of sound in CO_2+CH_3OH mixtures in this work, c, from the speed of sound in pure CO_2 calculated by the Span and Wagner EoS, c_{EoS}. ★, $x_{\mathrm{CO_2}} = 0.9503$; ◆, $x_{\mathrm{CO_2}} = 0.9700$; ▲, $x_{\mathrm{CO_2}} = 0.9794$; ●, $x_{\mathrm{CO_2}} = 0.9845$; ■, $x_{\mathrm{CO_2}} = 0.9898$. Deviations when doping with 1% of methanol lie between the dotted lines.

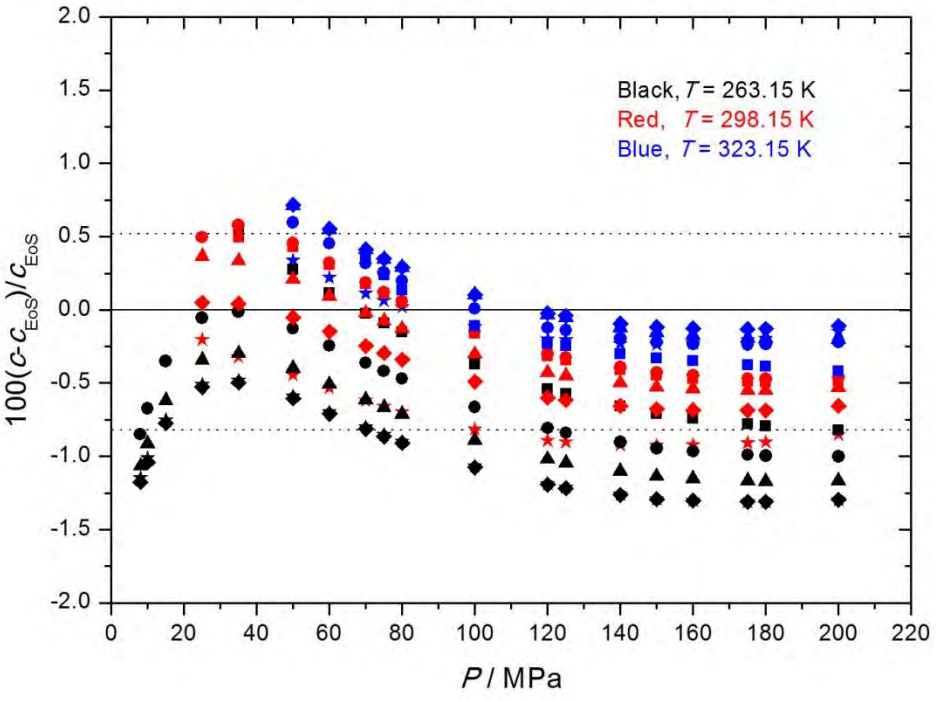

Figure 9. Correlation of the speed of sound calculated with equation (7), c_{fit}, as a function of the CO_2 mole fraction, x_{CO_2}, for the CO_2+CH_3OH mixtures at the three studied temperatures and at several pressures (equation 8, Table 9). ■, *P* = 50 MPa; ▲, *P* = 100 MPa; ◆, *P* = 150 MPa; ★, *P* = 200 MPa. Black, *T* = 263.15 K; red, *T* = 298.15 K; blue, *T* = 323.15 K.

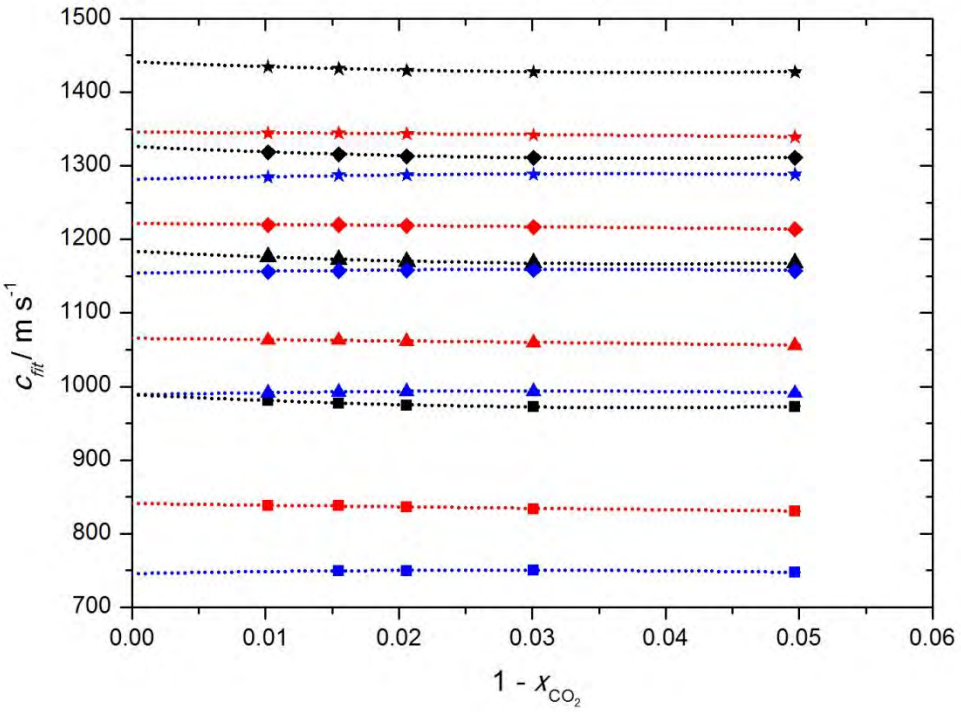

Figure 10. Relative deviations between the $P - c - T$ data in this work for the binary (c_{bin}) CO_2+SO_2 ($x_{CO_2} = 0.8969, x_{SO_2} = 0.1031$) and the ternary (c_{ter}) CO_2 + CH_3OH + SO_2 ($x_{CO_2} = 0.8889, x_{CH_3OH} = 0.0080, x_{SO_2} = 0.1031$) mixtures at temperatures T and pressures P. ■, T = 263.15 K; ●, T = 273.15 K; ▲, T = 293.15 K; ◆, T = 304.16 K; ▶, T = 313.15 K; ▼, T = 333.15 K; ◀, T = 353.15 K; ★, T = 373.19 K. Solid symbols, correlated data; empty symbols, extrapolated data (equation 7, Tables 7 and 8).

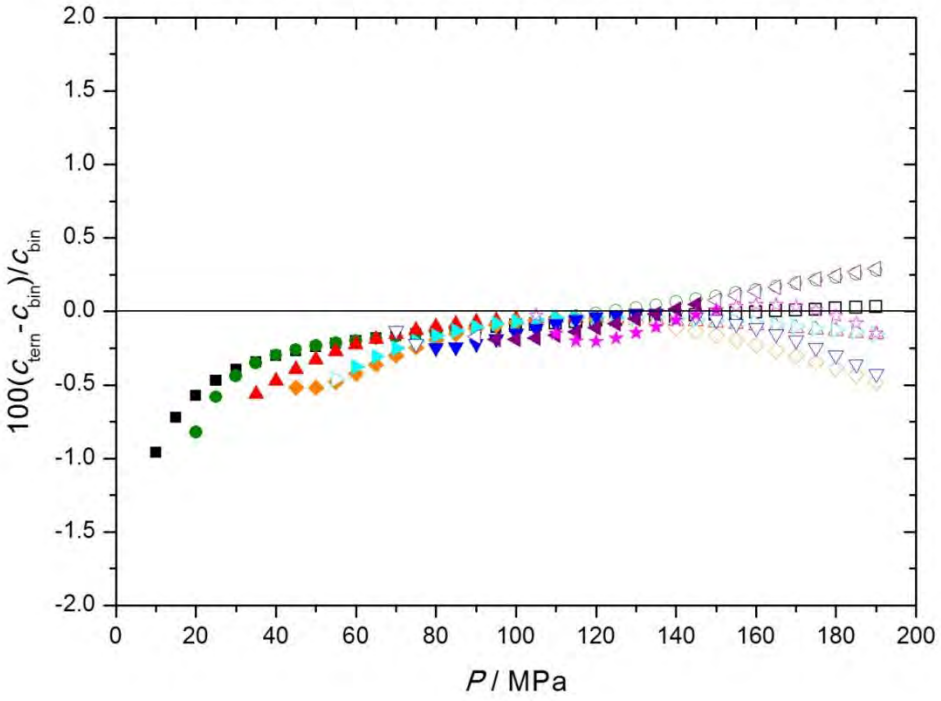

Figure

Figure 1. Speed of sound, c, in CO_2+CH_3OH with $x_{CO_2} = 0.9503$ at temperatures T and pressures P. Symbols, experimental points: ■, T = 263.15 K; ▲, T = 298.15 K; ★, T = 323.15 K. Solid lines, PC-SAFT EoS; dashed lines, REFPROP 9 software.

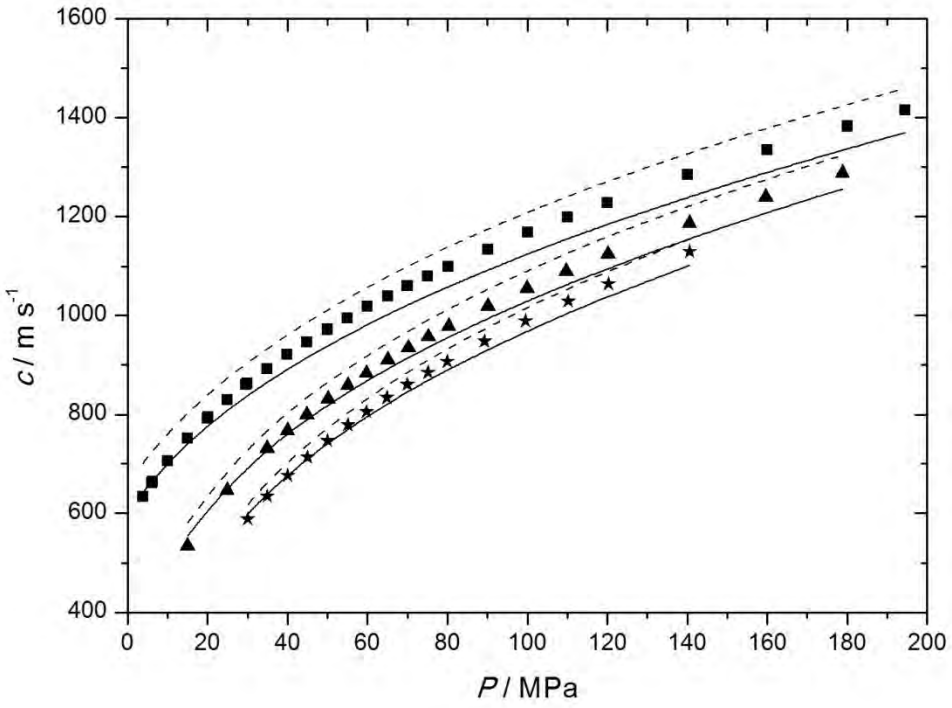

Figure 2. Relative deviations of the experimental speed of sound, c, from the values obtained from equation (7), c_{fit}, for all experimental points of the studied CO_2+CH_3OH mixtures. ■, T = 263.15 K; ▲, T = 298.15 K; ★, T = 323.15 K. The deviations of the data used in the section 5.1 range between -0.05% and +0.08% (dotted lines).

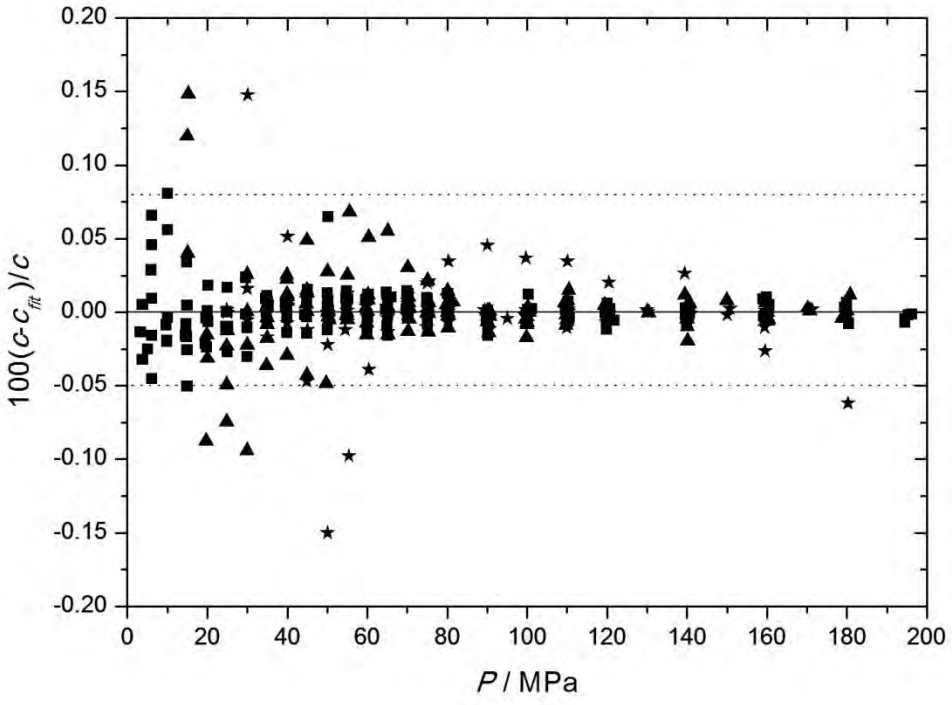

Figure 3. Speed of sound, c, in CO_2+SO_2 with $x_{CO_2} = 0.8969$ and $x_{SO_2} = 0.1031$ at temperatures T and pressures P. Symbols, experimental points: ■, T = 263.15 K; ▲, T = 293.15 K; ▼, T = 333.15 K; ★, T = 373.19 K. Solid lines, PC-SAFT EoS; dashed lines, REFPROP 9 software.

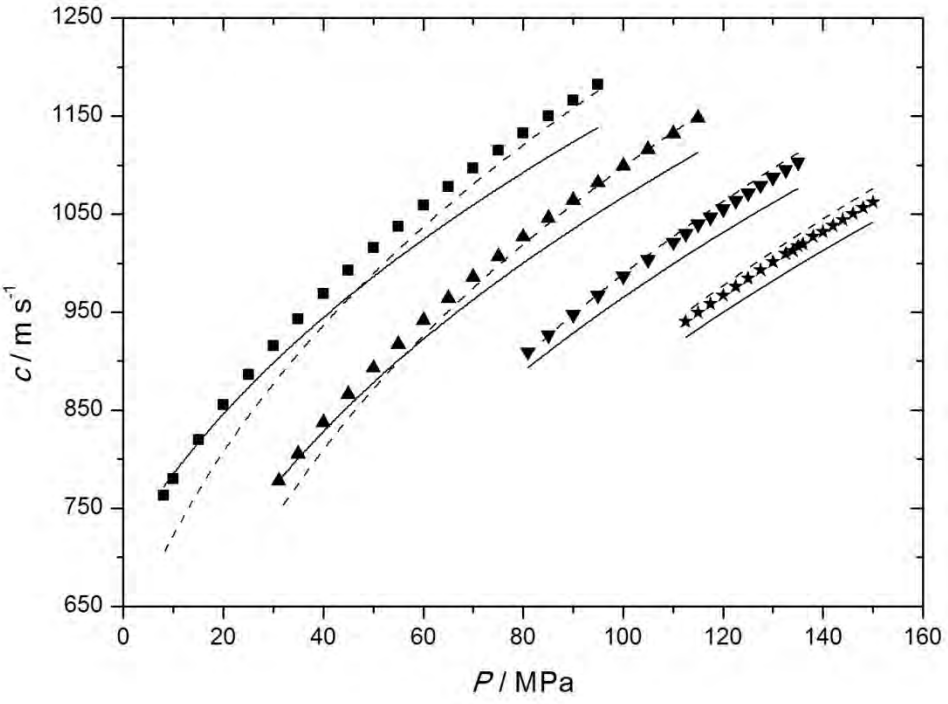

Figure 4. Speed of sound, c, in CO_2+CH_3OH+SO_2 with $x_{CO_2} = 0.8889$, $x_{CH_3OH} = 0.0080$ and $x_{SO_2} = 0.1031$ at temperatures T and pressures P. Symbols, experimental points: ■, T = 263.15 K; ▲, T = 293.15 K; ▼, T = 333.15 K; ★, T = 373.19 K. Solid lines, PC-SAFT EoS; dashed lines, REFPROP 9 software; system modeled as a binary mixture with $x_{CO_2} = 0.8989$, $x_{SO_2} = 0.1031$.

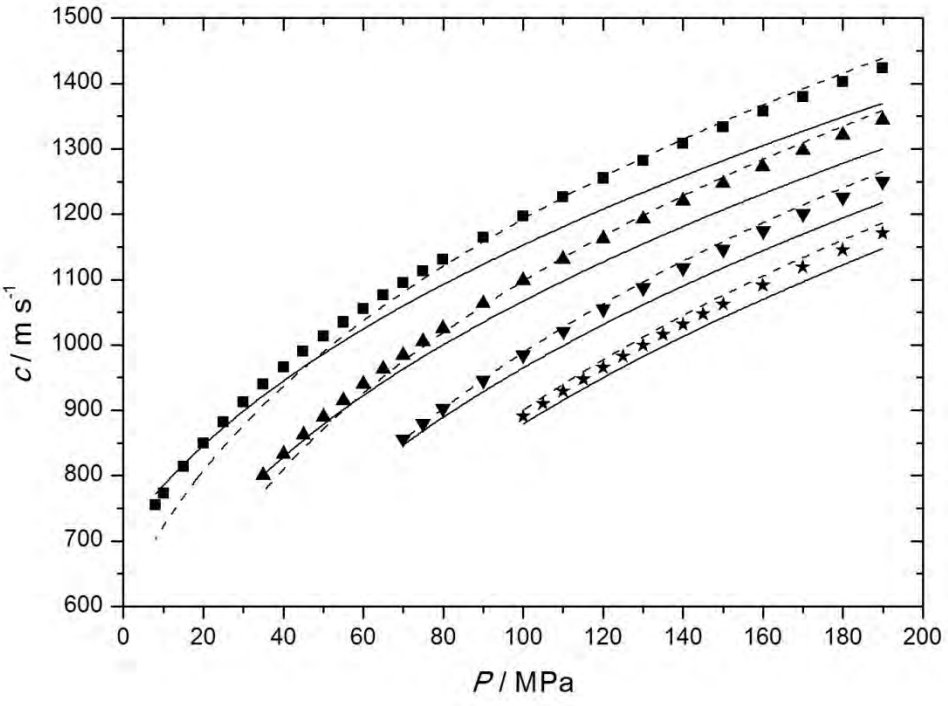

Figure 5. Speed of sound, c, in pure CO_2 versus pressure, P, at temperatures T. □, T = 263.15 K; △, T = 298.15 K; ○, T = 323.15 K.

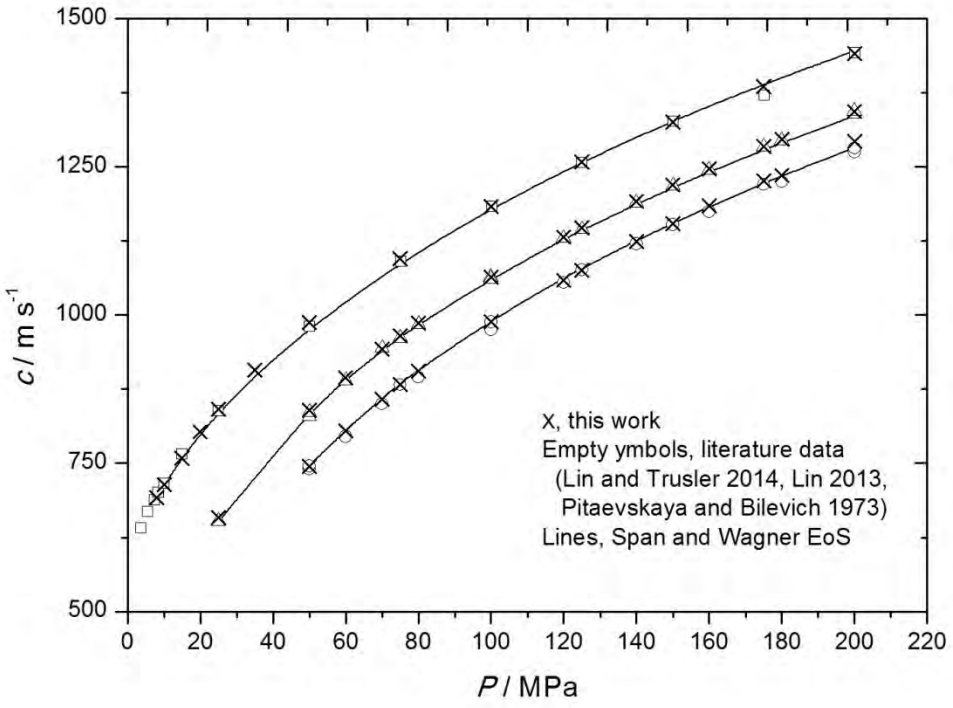

Figure 6. Speed of sound, c, in pure CO_2 versus temperature, T, at pressures P. □, P = 8 MPa; ○ , P = 15 MPa; △, P = 25 MPa; ▽, P = 50 MPa; ◇ , P = 75 MPa; ◁, P = 100 MPa; ▷, P = 125 MPa; ⊕, P = 150 MPa; ☆, P = 175 MPa; ☒, P = 200 MPa.

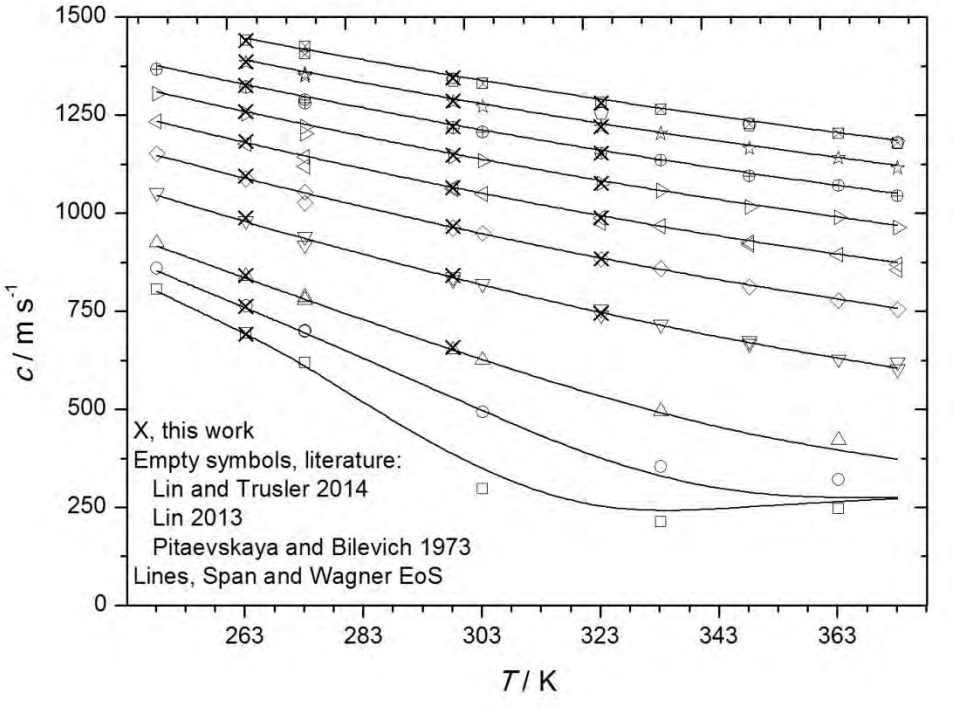

Figure 7. Relative deviations of the speed of sound in pure CO_2 obtained in this work and those in the literature, c, from the values obtained using the Span and Wagner EoS, c_{EoS}. □, T = 263.15 K; △, T = 298.15 K; ○, T = 323.15 K.

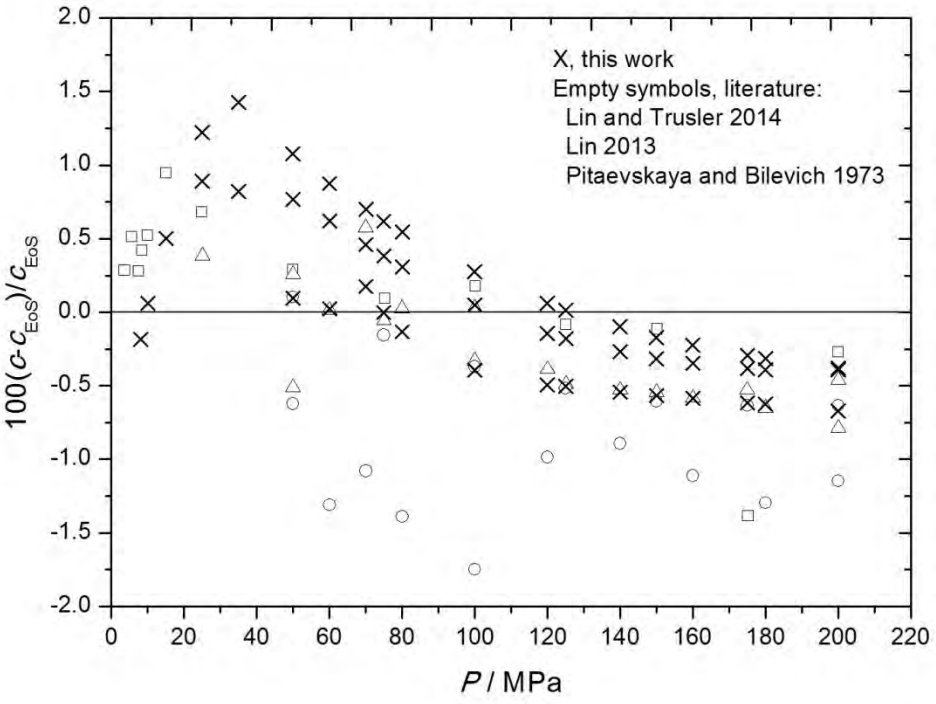

Figure 8. Relative deviations of the experimental speed of sound in CO_2+CH_3OH mixtures in this work, c, from the speed of sound in pure CO_2 calculated by the Span and Wagner EoS, c_{EoS}. ★, $x_{\mathrm{CO_2}} = 0.9503$; ◆, $x_{\mathrm{CO_2}} = 0.9700$; ▲, $x_{\mathrm{CO_2}} = 0.9794$; ●, $x_{\mathrm{CO_2}} = 0.9845$; ■, $x_{\mathrm{CO_2}} = 0.9898$. Deviations when doping with 1% of methanol lie between the dotted lines.

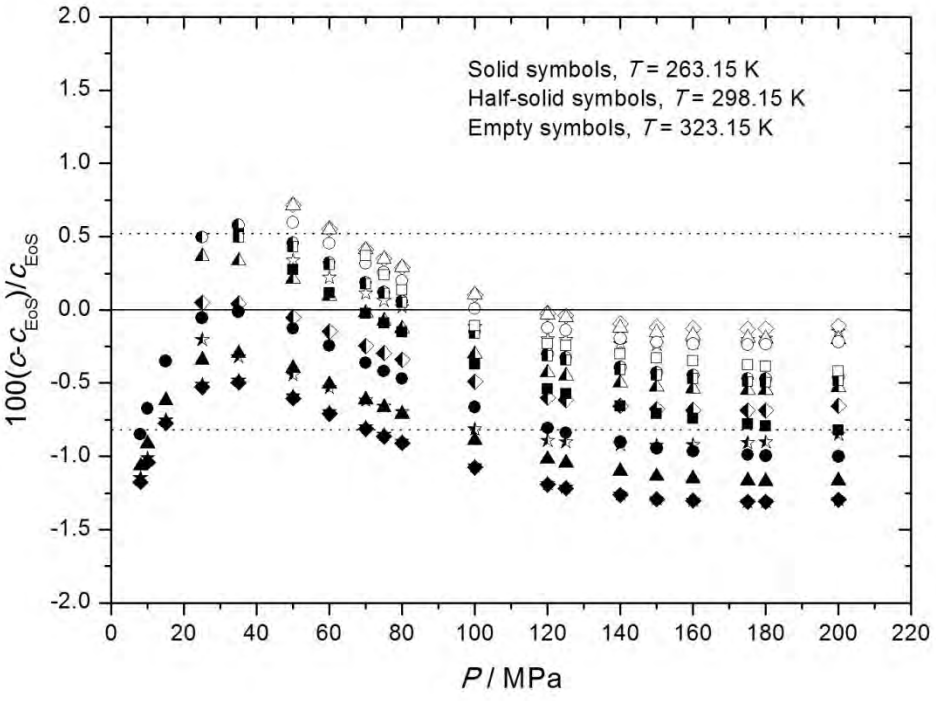

Figure 9. . Correlation of the speed of sound calculated with equation (7), c_{fit}, as a function of the CO_2 mole fraction, x_{CO_2}, for the CO_2+CH_3OH mixtures at the three studied temperatures and at several pressures (equation 8, Table 9). ■, *P* = 50 MPa; ▲, *P* = 100 MPa; ◆, *P* = 150 MPa; ★, *P* = 200 MPa. Solid symbols, *T* = 263.15 K; half-solid symbols, *T* = 298.15 K; empty symbols, *T* = 323.15 K.

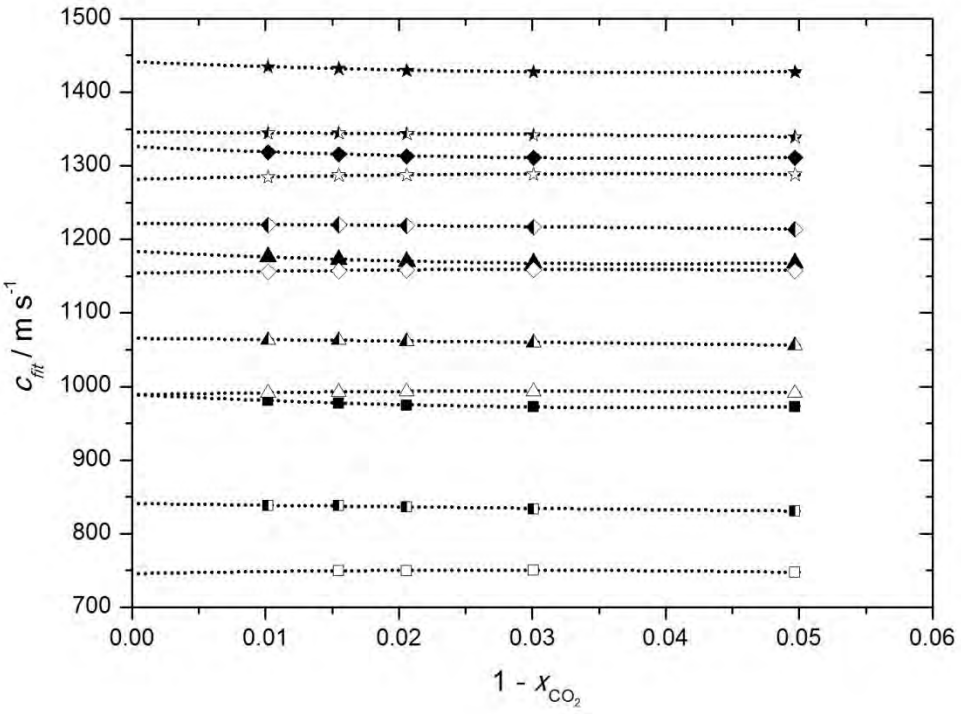

Figure 10. Relative deviations between the $P - c - T$ data in this work for the binary (c_{bin}) CO_2+SO_2 ($x_{CO_2} = 0.8969, x_{SO_2} = 0.1031$) and the ternary (c_{ter}) CO_2 + CH_3OH + SO_2 ($x_{CO_2} = 0.8889$, $x_{CH_3OH} = 0.0080$, $x_{SO_2} = 0.1031$) mixtures at temperatures T and pressures P. ■, T = 263.15 K; ●, T = 273.15 K; ▲, T = 293.15 K; ◆, T = 304.16 K; ▶, T = 313.15 K; ▼, T = 333.15 K; ◀, T = 353.15 K; ★, T = 373.19 K. Solid symbols, correlated data; empty symbols, extrapolated data (equation 7, Tables 7 and 8).

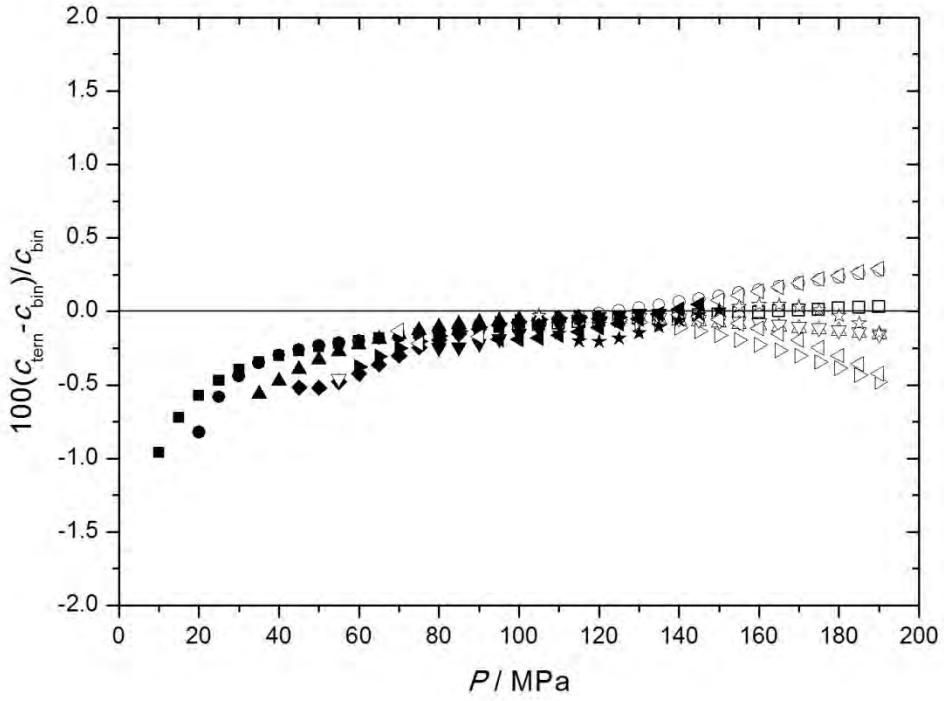

High-pressure speed of sound in pure CO_2 and in CO_2 with SO_2 as an impurity using methanol as a doping agent

Clara Rivas, Beatriz Gimeno, Manuela Artal, Sofía T. Blanco, Javier Fernández , Inmaculada Velasco*

Departamento de Química Física, Facultad de Ciencias, Universidad de Zaragoza, 50009 – Zaragoza, Spain

*Corresponding author: curra@unizar.es

SUPPLEMENTARY MATERIAL

TABLE OF CONTENTS

the CO_2+CH_3OH+SO_2 mixture with $x_{CO_2} = 0.8889$, $x_{CH_3OH} = 0.0080$ and $x_{SO_2} = 0.1031$ and the values calculated using the PC-SAFT EoS and the REFPROP 9 software, modeled as a binary mixture.	

Table S1. Parameters used in the modeling of the studied systems with the PC-SAFT EoS.

CO_2+CH_3OH and CO_2+CH_3OH+SO_2 systems			
Pure compound parameters	CO_2 [a]	CH_3OH [a]	SO2 [b]
m/M (mol/g)	0.04834	0.05273	0.04466
σ (Å)	2.8251	3.3264	2.6826
ε (K)	163.76	175.20	205.35
$\kappa^{A_iB_i}$	0.035176	0.035176	
$\varepsilon^{A_iB_i}$ (K)	0	2899.5	
Association scheme	2C	2B	
CO_2+SO_2 system			
Pure compound parameters	CO_2 [b]		SO2 [b]
m/M (mol/g)	0.04710		0.04466
σ (Å)	2.7852		2.6826
ε (K)	169.21		205.35
Binary interaction parameter CO_2 - CH_3OH [a]: $k_{ij} = -0.323 + 2.88 \times 10^{-4}\, T$			
Binary interaction parameter CO_2 – SO_2 [c]: $k_{ij} = 0.03$			
Binary interaction parameter SO_2 - CH_3OH [d]: $k_{ij} = 0$			

[a] Gil, L., Blanco, S., Rivas, C., Laga, E., Fernández, J., Artal, M., Velasco, I., 2012. Experimental determination of the critical loci for {*n*-C_6H_{14} or CO_2 + alkan-1-ol} mixtures. Evaluation of their critical and subcritical behavior using PC-SAFT EoS. The Journal of Supercritical Fluids 71, 26-44. http://dx.doi.org/10.1016/j.supflu.2012.07.008.

[b] Gross, J., Sadowski, G., 2001. Perturbed-Chain SAFT: An equation of state based on a perturbation theory for chain molecules. Industrial & Engineering Chemical Research 40, 1244-1260. http://dx.doi.org/10.1021/ie0003887.

[c] Diamantonis, N.I., Boulougouris, G.C., Mansoor, E.,Tsangaris, D.M., Economou, I.G., 2013. Evaluation of cubic, SAFT, and PC-SAFT equations of state for the vapor-liquid equilibrium modeling of CO_2 mixtures with other gases. Industrial & Engineering Chemistry Research 52, 3933-3942. http://dx.doi.org/10.1021/ie303248q.

[d] This work, T = 263.15-313.15 K.

Figure S1. Speed of sound, c, in CO_2+CH_3OH with $x_{CO_2} = 0.8005$ at temperatures T and pressures P. Symbols, experimental points: ■, T = 263.15 K; ▲, T = 298.15 K; ★, T = 323.15 K. Solid lines, PC-SAFT EoS; dashed lines, REFPROP 9 software.

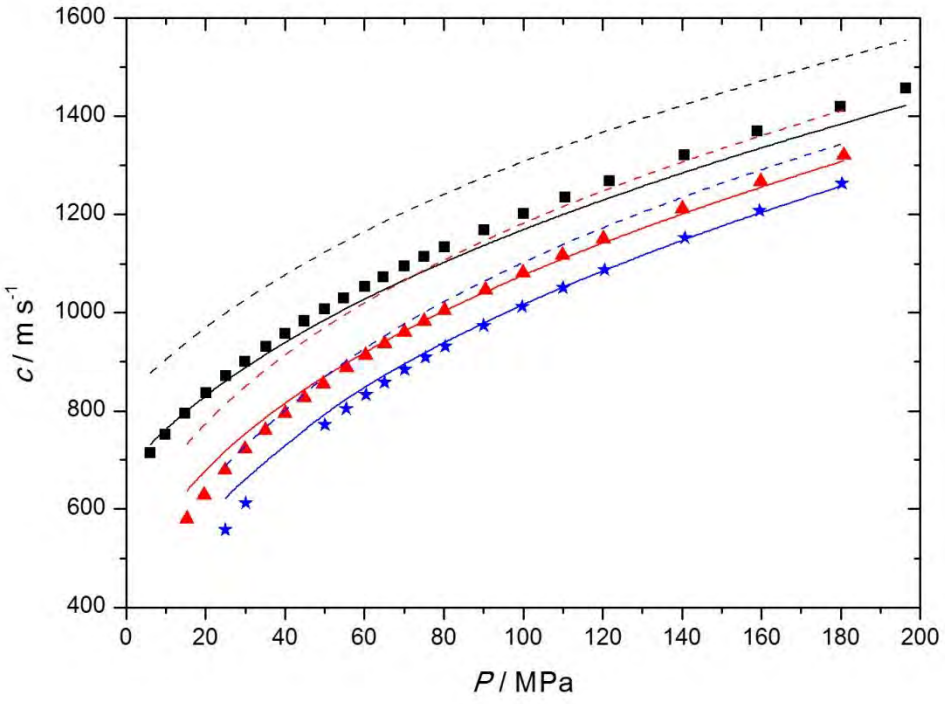

Figure S2. Speed of sound, c, in CO_2+CH_3OH with $x_{CO_2} = 0.9025$ at temperatures T and pressures P. Symbols, experimental points: ■, T = 263.15 K; ▲, T = 298.15 K; ★, T = 323.15 K. Solid lines, PC-SAFT EoS; dashed lines, REFPROP 9 software.

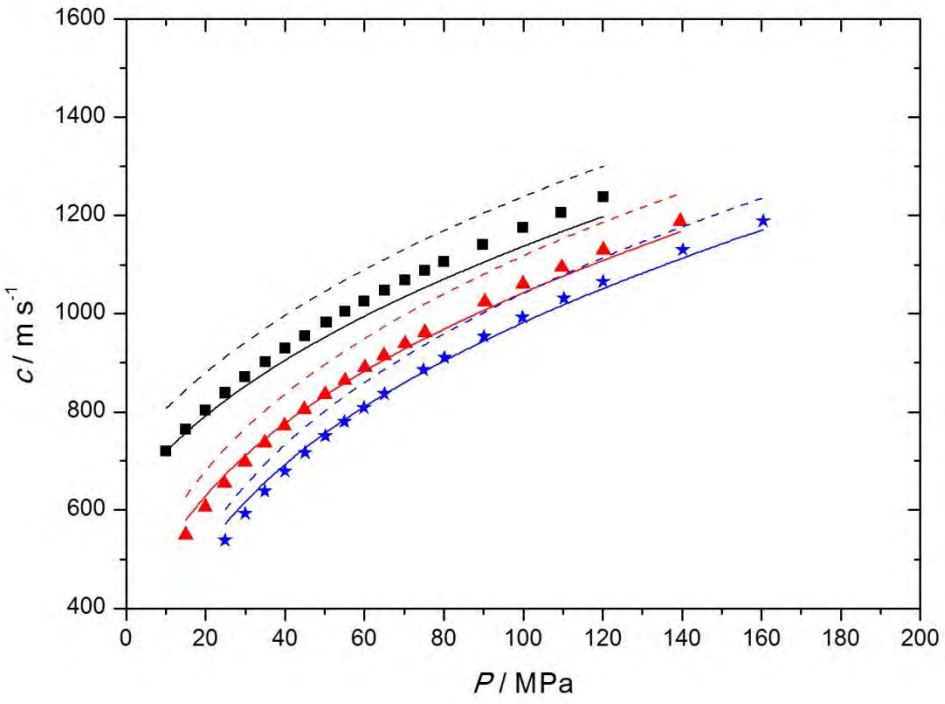

Figure S3. Speed of sound, c, in CO_2+CH_3OH with $x_{CO_2} = 0.9700$ at temperatures T and pressures P. Symbols, experimental points: ■, T = 263.15 K (Rivas et al. 2016); ▲, T = 298.15 K; ★, T = 323.15 K. Solid lines, PC-SAFT EoS; dashed lines, REFPROP 9 software.

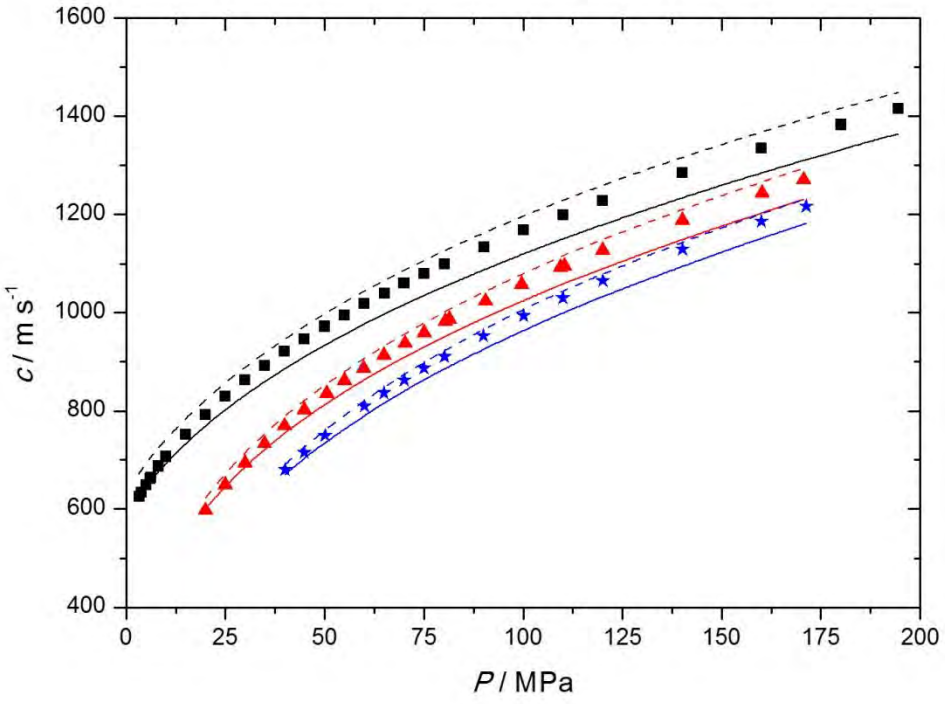

Figure S4. Speed of sound, c, in CO_2+CH_3OH with $x_{CO_2} = 0.9794$ at temperatures T and pressures P. Symbols, experimental points: ■, T = 263.15 K; ▲, T = 298.15 K; ★, T = 323.15 K. Solid lines, PC-SAFT EoS; dashed lines, REFPROP 9 software.

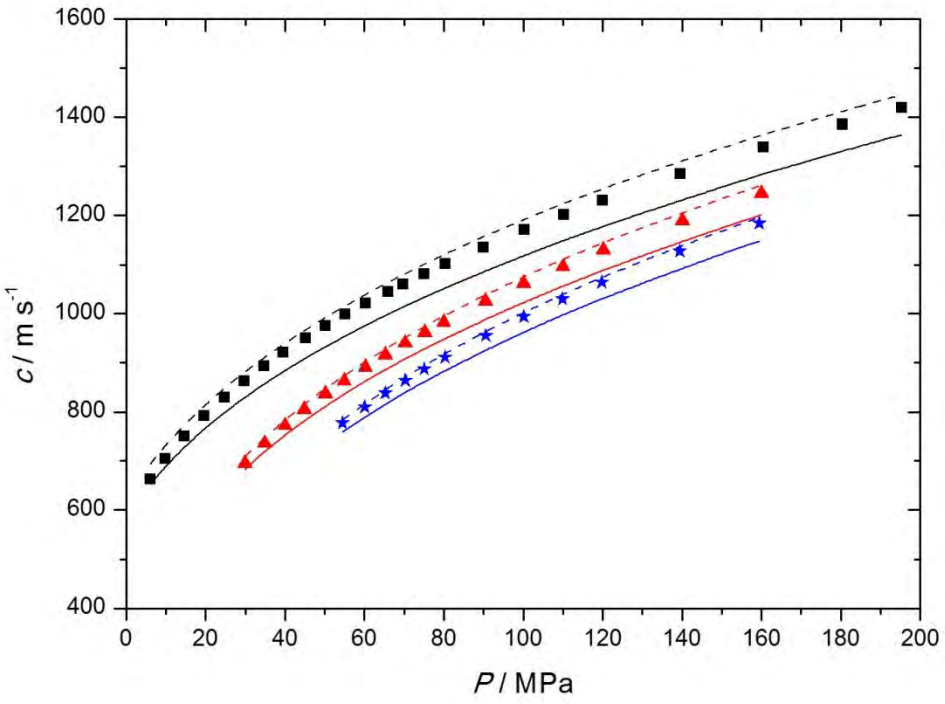

Figure S5. Speed of sound, c, in CO_2+CH_3OH with $x_{CO_2} = 0.9845$ at temperatures T and pressures P. Symbols, experimental points: ■, T = 263.15 K; ▲, T = 298.15 K; ★, T = 323.15 K. Solid lines, PC-SAFT EoS; dashed lines, REFPROP 9 software.

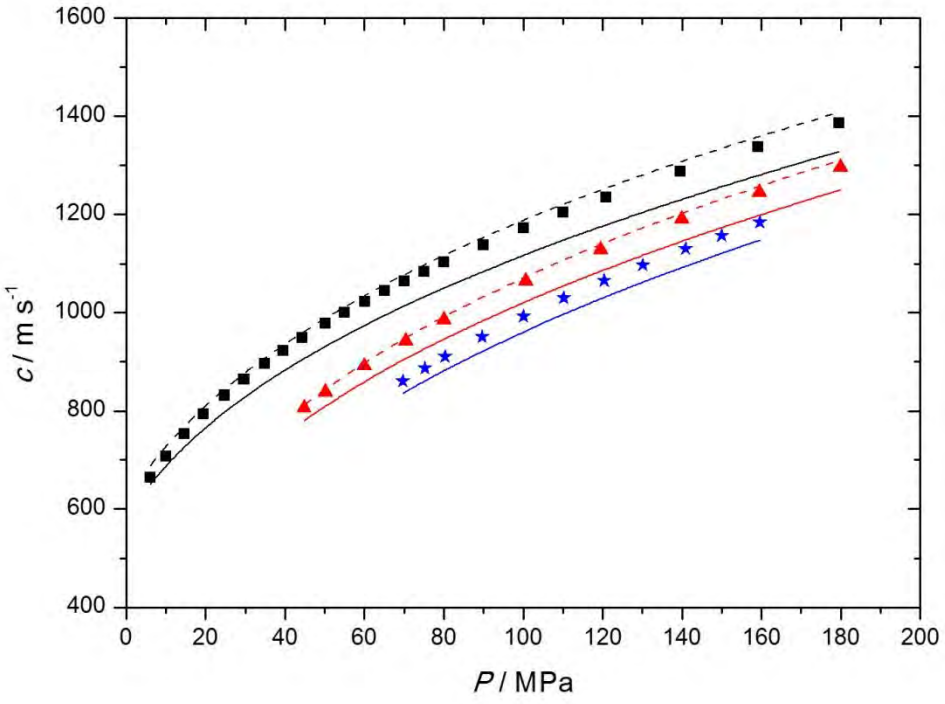

Figure S6. Speed of sound, c, in CO_2+CH_3OH with $x_{CO_2} = 0.9898$ at temperatures T and pressures P. Symbols, experimental points: ■, T = 263.15 K; ▲, T = 298.15 K; ★, T = 323.15 K. Solid lines, PC-SAFT EoS; dashed lines, REFPROP 9 software.

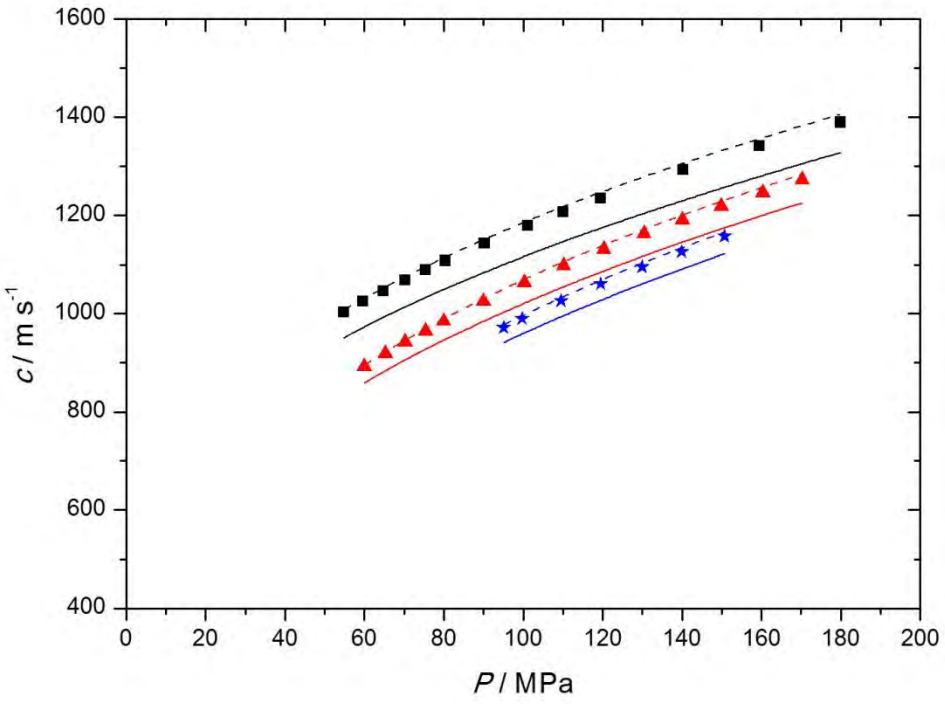

Figure S7. Relative deviations between the experimental speed of sound in this work in the CO_2+CH_3OH mixtures, c, and the values calculated using the PC-SAFT EoS and the REFPROP 9 software, c_{model}, at T = 263.15 K.

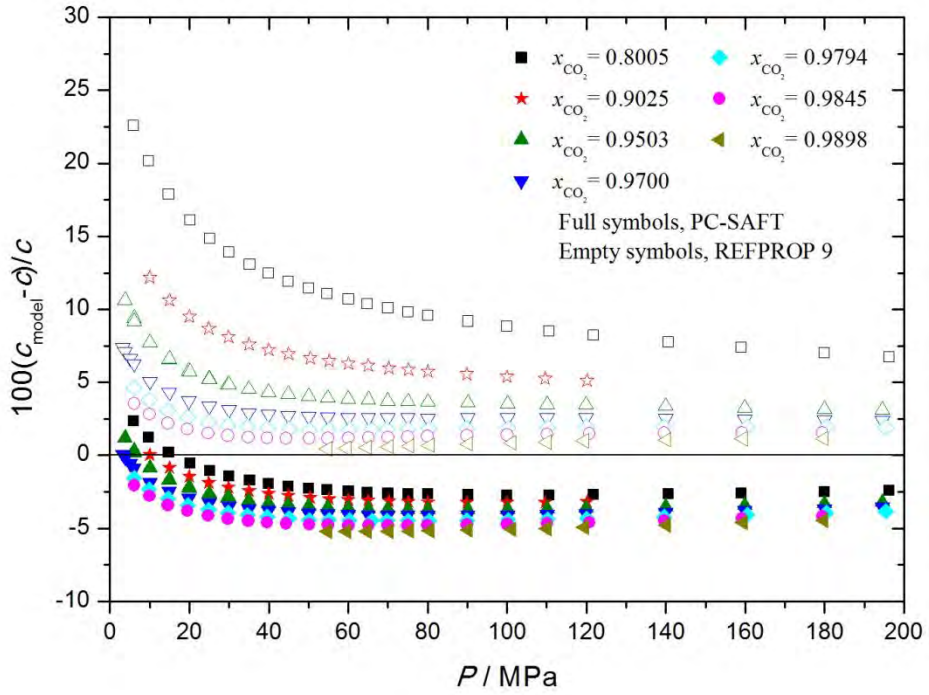

Figure S8. Relative deviations between the experimental speed of sound in this work in the CO_2+CH_3OH mixtures, c, and the values calculated using the PC-SAFT EoS and the REFPROP 9 software, c_{model}, at T = 298.15 K.

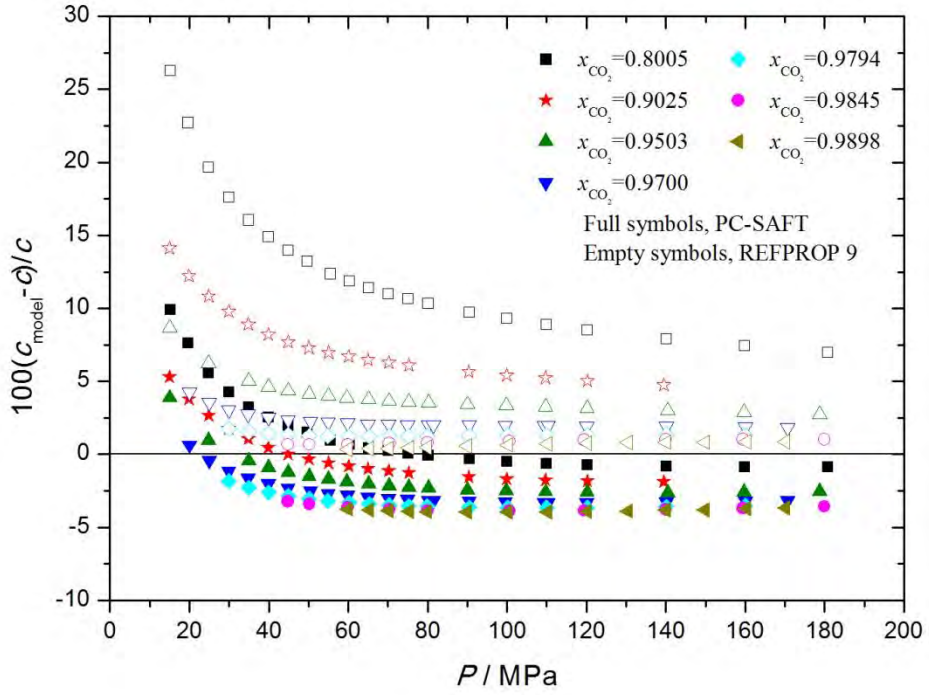

Figure S9. Relative deviations between the experimental speed of sound in this work in the CO_2+CH_3OH mixtures, c, and the values calculated using the PC-SAFT EoS and the REFPROP 9 software, c_{model}, at T = 323.15 K.

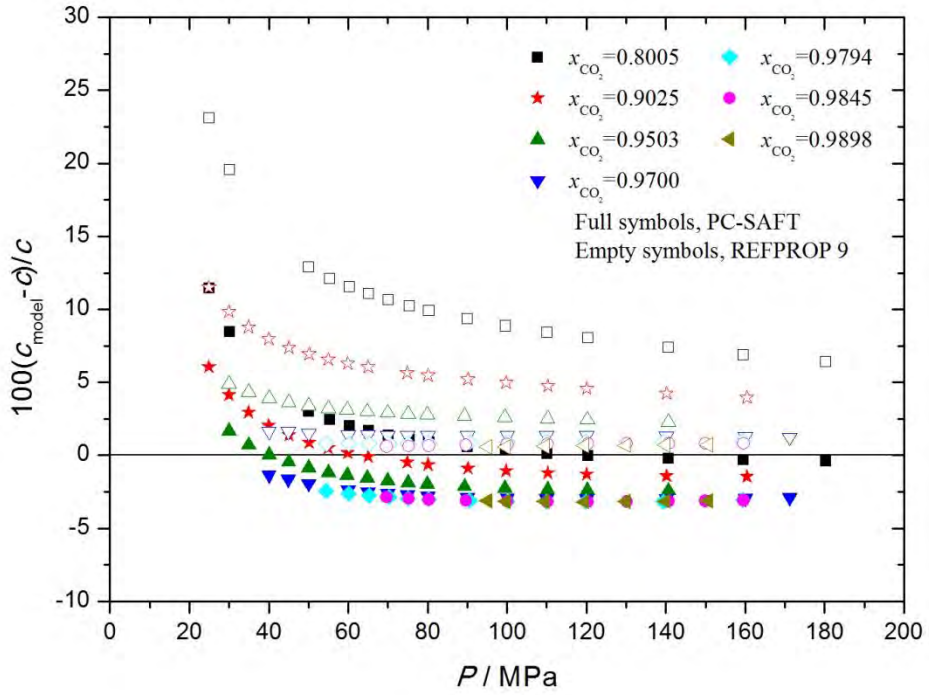

Figure S10. Relative deviations between the experimental speed of sound in this work in the CO_2+SO_2 mixture with $x_{CO_2} = 0.8969$ and $x_{SO_2} = 0.1031$, c, and the values calculated using the PC-SAFT EoS and the REFPROP 9 software, c_{model}, at temperatures T.

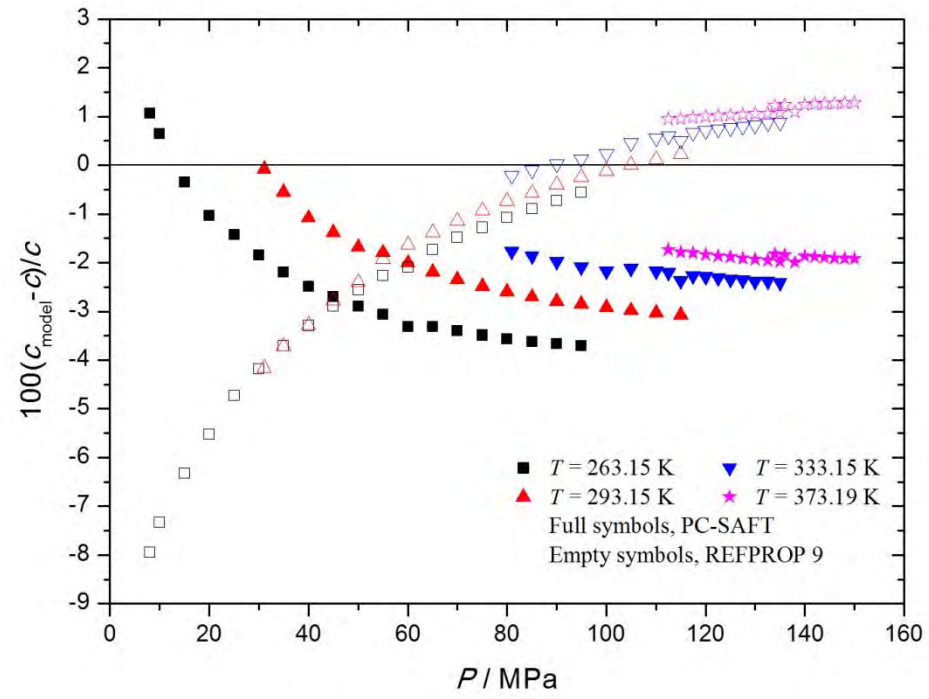

Figure S11. Speed of sound, c, in CO_2+CH_3OH+SO_2 with $x_{CO_2} = 0.8889$, $x_{CH_3OH} = 0.0080$ and $x_{SO_2} = 0.1031$ at temperatures T and pressures P. Symbols, experimental points: ■, T = 263.15 K; ▲, T = 293.15 K; ▼, T = 333.15 K; ★, T = 373.15 K. Solid lines, PC-SAFT EoS; dashed lines, REFPROP 9 software; system modeled as a ternary mixture.

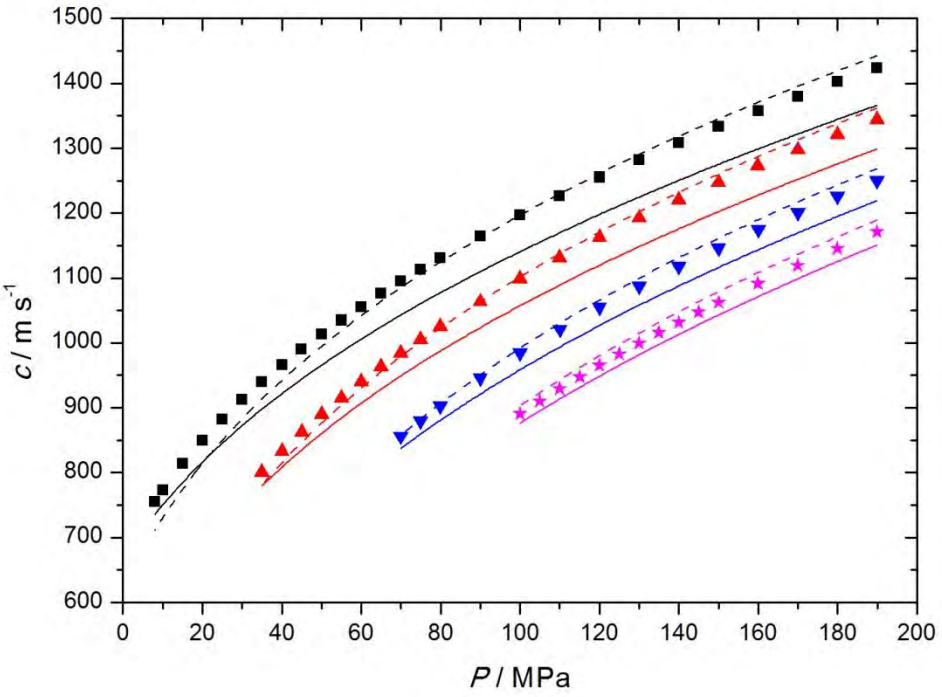

Figure S12. Relative deviations between the experimental speed of sound in this work in the CO_2+CH_3OH+SO_2 mixture with $x_{CO_2} = 0.8889$, $x_{CH_3OH} = 0.0080$ and $x_{SO_2} = 0.1031$, c, and the values calculated using the PC-SAFT EoS and the REFPROP 9 software, c_{model}, at temperatures T. The system was modeled as a ternary mixture.

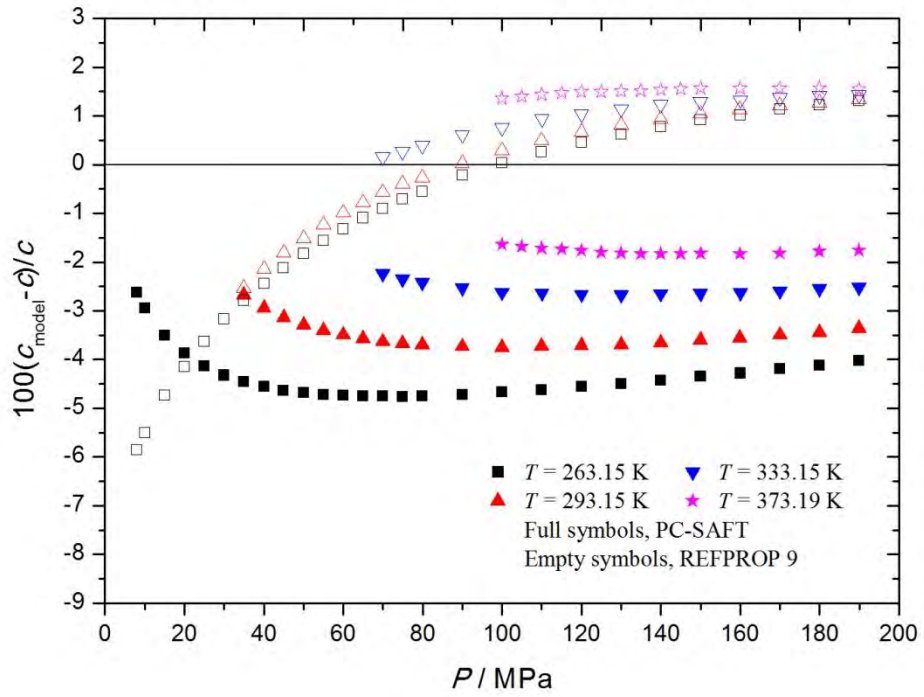

Figure S13. Relative deviations between the experimental speed of sound in the present work in the CO_2+CH_3OH+SO_2 mixture with $x_{CO_2} = 0.8889$, $x_{CH_3OH} = 0.0080$ and $x_{SO_2} = 0.1031$, c, and the values calculated using the PC-SAFT EoS and the REFPROP 9 software, c_{model}, at temperatures T. The system was modeled as a binary mixture with $x_{CO_2} = 0.8969$ and $x_{SO_2} = 0.1031$.

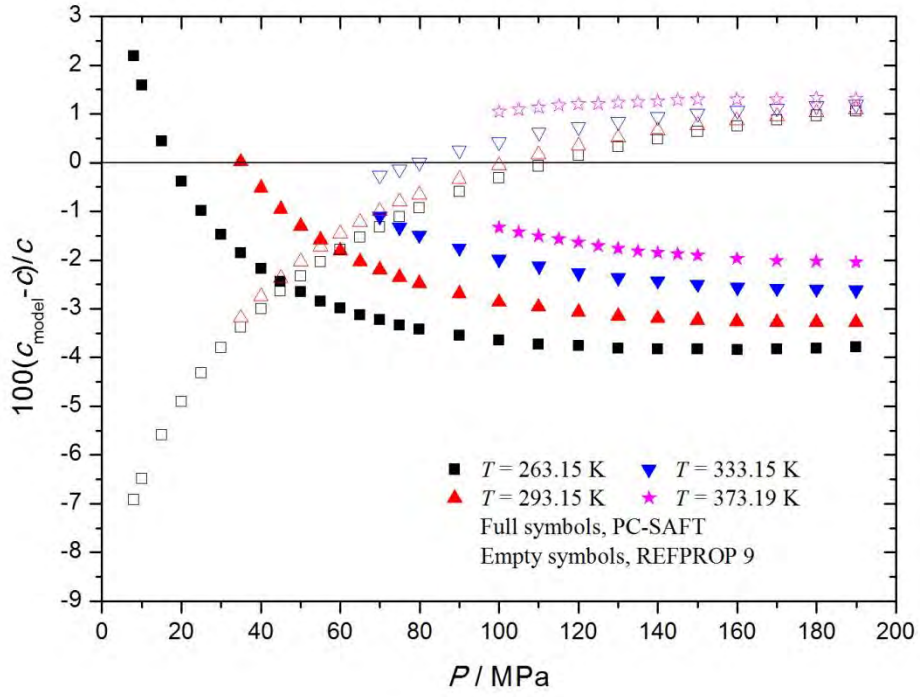

Graphical Abstract